Heterogeneous N_2O_5 uptake coefficient and production yield of $ClNO_2$ in polluted northern China: Roles of aerosol water content and chemical composition

Yee Jun Tham[1,2], Zhe Wang[1], Qinyi Li[1a], Weihao Wang[1], Xinfeng Wang[3], Keding Lu[4], Nan Ma[5], Chao Yan[2], Simonas Kecorius[5], Alfred Wiedensohler[5], Yuanhang Zhang[4], and Tao Wang[1]

[1]Department of Civil and Environmental Engineering, The Hong Kong Polytechnic University, Hong Kong, China
[2]Institute for Atmospheric and Earth System Research/Physics, University of Helsinki, 00014, Helsinki, Finland
[3]Environment Research Institute, Shandong University, Jinan, Shandong, China
[4]State Key Joint Laboratory of Environmental Simulation and Pollution Control, College of Environmental Sciences and Engineering, Peking University, Beijing, China
[5]Leibniz Institute for Tropospheric Research, Permoserstr. 15, 04318 Leipzig, Germany
[a]Now at: Department of Atmospheric Chemistry and Climate, Institute of Physical Chemistry Rocasolano, CSIC, Madrid 28006, Spain.

Correspondence to: Z. Wang (z.wang@polyu.edu.hk) and T. Wang (cetwang@polyu.edu.hk)

Abstract. Heterogeneous uptake of dinitrogen pentoxide (N_2O_5) and production of nitryl chloride ($ClNO_2$) are important nocturnal atmospheric processes that have significant implications for the production of secondary pollutants. However, the understanding of N_2O_5 uptake processes and $ClNO_2$ production remains limited, especially in China. This study presents a field investigation of the N_2O_5 heterogeneous uptake coefficient ($\gamma(N_2O_5)$) and $ClNO_2$ production yield (ϕ) in a polluted area of northern China during the summer of 2014. The N_2O_5 uptake coefficient and $ClNO_2$ yield were estimated by using the simultaneously measured $ClNO_2$ and total nitrate in ten selected cases, which have concurrent increases in the $ClNO_2$ and nitrate concentrations and relatively stable environmental conditions. The determined $\gamma(N_2O_5)$ and ϕ values varied greatly, with an average of 0.022 for $\gamma(N_2O_5)$ (± 0.012, standard deviation) and 0.34 for ϕ (± 0.28, standard deviation). The variations in $\gamma(N_2O_5)$ could not be fully explained by the previously derived parameterizations of N_2O_5 uptake that consider nitrate, chloride, and the organic coating. Heterogeneous uptake of N_2O_5 was found to have a strong positive dependence on the relative humidity and aerosol water content. This result suggests that the heterogeneous uptake of N_2O_5 in Wangdu is governed mainly by the amount of water in the aerosol, and is strongly water limited, which is different from most of the field observations in the United States and Europe. The $ClNO_2$ yield estimated from the parameterization was also overestimated comparing to that derived from the observation. The observation-derived ϕ showed a decreasing trend with an increasing ratio of acetonitrile to carbon monoxide, an indicator of biomass burning emissions, which suggests a possible suppressive effect on the production yield of $ClNO_2$ in the plumes influenced by biomass burning in this region. The findings of this study illustrate the need to improve our understanding and to parameterize the key factors for $\gamma(N_2O_5)$ and ϕ to accurately assess the photochemical and haze pollution.

1 Introduction

The nocturnal heterogeneous reaction of dinitrogen pentoxide (N_2O_5) with aerosols is a loss pathway of NO_x and a source of aerosol nitrate and gas-phase nitryl chloride ($ClNO_2$) (Brown et al., 2006; Osthoff et al., 2008; Thornton et al., 2010; Sarwar et al., 2014) and thereby has important implications on air quality (e.g., Li et al., 2016; Tang et al., 2017). The process begins with the accumulation of gas-phase nitrate radical (NO_3) after sunset via the oxidation of nitrogen dioxide (NO_2) by O_3 and further reaction of NO_3 with another NO_2, yielding N_2O_5. The accommodation of N_2O_5 on the aqueous surface of the aerosol (R1) and reaction with liquid water (H_2O) leads to the formation of a protonated nitric acid intermediate ($H_2ONO_2^+$) and a nitrate (NO_3^-) (R2; Thornton and Abbatt, 2005; Bertram and Thornton, 2009).

$$N_2O_5\ (g) \leftrightharpoons N_2O_5\ (aq) \qquad (R1)$$

$$N_2O_5\ (aq) + H_2O\ (l) \leftrightharpoons NO_3^-(aq) + H_2ONO_2^+(aq) \qquad (R2)$$

The $H_2ONO_2^+$ will proceed by reacting with another H_2O to form an aqueous nitric acid (HNO_3; R3). If chloride (Cl^-) is present in the aerosols, the $H_2ONO_2^+$ will undergo another pathway to produce a nitryl chloride ($ClNO_2$) through R4, which is a dominant source of highly reactive chlorine radicals in the troposphere (e.g., Riedel et al., 2012a; 2014).

$$H_2ONO_2^+(aq) + H_2O\ (l) \rightarrow H_3O^+(aq) + HNO_3(aq) \qquad (R3)$$

$$H_2ONO_2^-(aq) + Cl^-(aq) \rightarrow ClNO_2 + H_2O(l) \qquad (R4)$$

The heterogeneous loss rate of N_2O_5 ($k(N_2O_5)_{het}$) and the $ClNO_2$ production rate ($p(ClNO_2)$) are fundamentally governed by the probability of N_2O_5 lost upon collision with particle surface area in a volume of air (i.e., uptake coefficient, $\gamma(N_2O_5)$) and the $ClNO_2$ yield (ϕ), which is defined as the branching ratio between the formation of HNO_3 via R3 and $ClNO_2$ via R4. Assuming that the gas-phase diffusion to the aerosol surfaces is negligible, their relationship can be described by equations (1) and (2), in which c_{N2O5} is the average molecular speed of N_2O_5 and S_a is the aerosol surface area.

$$k(N_2O_5)_{het} = \frac{1}{4} c_{N2O5}\gamma(N_2O_5)S_a \qquad (Eq\ 1)$$

$$p(ClNO_2) = k(N_2O_5)_{het}[N_2O_5]\phi \qquad (Eq\ 2)$$

N_2O_5 uptake has been shown in the laboratory to be susceptible to changes in the water content, chloride, nitrate, and organic particle coatings in aerosols (e.g., Mentel et al., 1999; Bertram and Thornton, 2009; Tang et al., 2014). The presence of liquid water on the aerosols allows the accommodation of N_2O_5 (R1) and acts as a medium for the solvation process of N_2O_5 (R2). It has been found that N_2O_5 uptake is significantly enhanced in humid conditions than in dry conditions (e.g., Hallquist et al., 2003; Bertram and Thornton, 2009; Gržinic et al., 2015). Higher loading of NO_3^- in the aerosol can dramatically decrease N_2O_5 uptake by reversing the solvation/ionization process of N_2O_5, shifting the equilibrium in R2 to the left to reproduce N_2O_5, which can be diffused out of the aerosol (known as the "nitrate suppression" effect). The rate of reversible reaction of R2 (i.e., $H_2ONO_2^+$ with NO_3^-) was documented to be 30 to 40 times faster than the reaction of $H_2ONO_2^+$ with liquid water in R3

(Bertram and Thornton, 2009; Griffiths et al., 2009). The presence of Cl^- in the aerosol, in contrast, can enhance the reactive uptake because Cl^- reacts effectively with $H_2ONO_2^+$ (in R4), thus negating the "nitrate suppression" effect by shifting the equilibrium in R2 to the right (Finlayson-Pitts et al., 1989; Bertram and Thornton, 2009). The uptake of N_2O_5 can also be hindered by the presence of organics, because the organic coating layer on the aerosol could lower the liquid water content and/or limit the surface activity, thus suppressing the accommodation of N_2O_5 (e.g., Cosman et al., 2008; Gaston et al., 2014).

As for the $ClNO_2$ yield from N_2O_5 heterogeneous reactions, it was found to be dependent on the fate of $H_2ONO_2^+$ and thus on the relative amount of Cl^- and water content (Benhke et al., 1997; Roberts et al., 2009; Bertram and Thornton, 2009). Therefore, ϕ can be expressed by the following equation (Eq.3).

$$\phi_{\text{param.}} = \frac{1}{\frac{k_{R3}[H_2O]}{k_{R4}[Cl^-]} + 1} \qquad \text{(Eq 3)}$$

Roberts et al. (2009) and reference therein reported that the coefficient rate of k_{R4} is about 450 - 836 times faster than that of k_{R3}, indicating that $H_2ONO_2^+$ proceeds more favorably via R4, even with a small amount of Cl^-. However, some laboratory experiments have suggested that the presence of halides (i.e., bromide), phenols, and humic acid may significantly reduce the ϕ (e.g., Schweitzer et al., 1998; Ryder et al., 2015).

The parameterization of $\gamma(N_2O_5)$ and ϕ as a function of the aerosol water content and aerosol chemical composition, derived based on the findings of the laboratory studies mentioned above (e.g., Antilla et al., 2006; Bertram and Thornton, 2009; Davis et al., 2008), has recently been compared with the ambient observations in different environments (Morgan et al., 2015; Phillips et al., 2016; Chang et al., 2016; Wang Z. et al., 2017; McDuffie et al., 2018). Large discrepancies were observed between the $\gamma(N_2O_5)$ and ϕ values determined in the fields and the laboratory parameterizations derived with pure or mixed aerosol samples, and the differences can be up to an order of magnitude. Several reasons have been proposed for the discrepancies between the parameterization and observation values, including the failure of parameterization to account for 1) the complex mixture of organic composition (Bertram et al., 2009; Mielke et al., 2013); 2) the "real" nitrate suppression effect (Riedel et al., 2012b; Morgan et al., 2015); 3) the varying mixing states of the particles (Ryder et al., 2014; Wang X. et al., 2017); and 4) bulk or surface reactions on different particles (e.g., Gaston and Thornton, 2016). These results suggest the lack of comprehensive understanding of the N_2O_5 uptake and $ClNO_2$ production yield in various atmospheric environments around the world.

Most of the previous field studies of N_2O_5 uptake and $ClNO_2$ production have been conducted in the United States (US) and Europe regions (Brown et al., 2009; Chang et al., 2016). Direct field investigation of the N_2O_5 heterogeneous processes in China is very limited. Pathak et al. (2009, 2011) analyzed the aerosol composition and suggested that the accumulation of fine NO_3^- aerosol downwind of Beijing and Shanghai was due to significant N_2O_5 heterogeneous reactions. Wang et al. (2013)

linked the observed NO_3^- with the precursors of N_2O_5 (i.e., NO_2 and O_3) in urban Shanghai and suggested that the N_2O_5 heterogeneous uptake dominated NO_3^- formation on polluted days. However, field measurements of N_2O_5 and $ClNO_2$ were not available until recently at several sites in southern and northern China (Tham et al., 2014; Wang Z. et al., 2017).

In the summer of 2014, a field campaign was carried out to investigate $ClNO_2$ and N_2O_5 at a semirural ground site at Wangdu in polluted northern China (Tham et al., 2016). Elevated levels of $ClNO_2$ up to 2070 pptv (1 min-average), but relatively low values of N_2O_5 (1 min-average maximum of 430 pptv), were observed on most nights at this site, and heterogeneous processes have been shown to have a significant effect on the following day's radical and ozone production at the site (Tham et al., 2016). Yet, the factors that drive the N_2O_5 heterogeneous uptake and $ClNO_2$ production yield remain unclear. In this study, we further analyze the dataset to investigate this topic. We first derive values for $\gamma(N_2O_5)$ and ϕ from the regression analysis of $ClNO_2$ and total nitrate (HNO_3 and particulate NO_3^-) dataset and then compare the values obtained in the field with various parameterizations derived from the laboratory studies. With the aid of the aerosol composition and meteorological measurements, we illustrate the factors that drive or influence the variations in $\gamma(N_2O_5)$ and ϕ at Wangdu. The values for $\gamma(N_2O_5)$ and ϕ obtained here are also compared with field results from the literature to provide an overview of the N_2O_5-$ClNO_2$ heterogeneous process observed in various environments around the world.

2 Methods

The measurement site (38.66°N, 115.204°E) is located at a semirural area in Wangdu county of Hebei province, in the northern part of China. The Wangdu site is situated within the agricultural land but is bounded by villages and towns. Beijing (the national capital) is about 170 km to the northeast, Tianjin is about 180 km to the east, Shijiazhuang is about 90 km to the southwest, and Baoding is ~33 km to the northeast. Dozens of major coal-fired power stations are also located in the region. During the study period, frequent biomass burning activity was observed in the surrounding regions. Analysis of the air masses' back trajectories showed that the sampling site was frequently affected by these surrounding anthropogenic sources. Details on the sampling site and the meteorological conditions during the campaign can be found in Tham et al. (2016).

In this study, N_2O_5 and $ClNO_2$ were measured with an iodide chemical mass ionization mass spectrometer (CIMS), with which the N_2O_5 and $ClNO_2$ were detected as the iodide-cluster ions of $I(ClNO_2)^-$ and $I(N_2O_5)^-$, similar to those outlined by Kercher et al. (2009). The detection principles, calibration, and inlet maintenance were described in detail in our previous studies (Wang T. et al., 2016; Tham et al., 2016). The CIMS measurement at the Wangdu site was performed from 20 June to 9 July 2014. A corona discharge ion source setup (for generation of iodide primary ions) was used in the CIMS measurement from 20 to 26 June 2014 with a detection limit of 16 pptv for N_2O_5 and 14 pptv for $ClNO_2$ (3σ; 1 min-averaged data) but was replaced by a radioactive ion source from 27 June 2014 until the end of the study with a detection limit of 7 pptv for N_2O_5 and

6 pptv for $ClNO_2$ (3σ; 1 min-averaged data). The overall uncertainty of the CIMS measurement was estimated to be ±25%, with a precision of 3%.

The present study was supported by other auxiliary measurements of aerosol, trace gases and meteorological parameters, and the detailed instrumentation for these measurements has been listed in a previous paper (Tham et al., 2016). Trace gases including NO, NO_2, O_3, SO_2, CO, and total odd nitrogen (NO_y) were measured with online gas analyzers (Tan et al., 2017). A gas aerosol collector–ion chromatography system was used to measure the ionic compositions of $PM_{2.5}$, including NO_3^-, Cl^-, SO_4^-, NH_4^+, and gas-phase HNO_3 (Dong et al., 2012). The particle surface area concentrations (S_a) were calculated based on the wet ambient particle number size distribution by assuming spherical particles. In brief, dry-state particle number size distribution was measured with a mobility particle size spectrometer (covering mobility particle diameter of 4 to 800 nm) and an aerodynamic particle size spectrometer (for aerodynamic particle diameter 0.8 to 10 µm). The wet particle number size distribution as a function of the relative humidity was calculated from a size-resolved kappa-Köhler function determined from real-time measurement of a High Humidity Tandem Differential Mobility Analyzer (Hennig et al., 2005; Liu et al., 2014). It should be noted that the major uncertainty of S_a calculation was the assumption and application of κ at different size-range, leading to an overall uncertainty of ±19%.

Hydroxyl radical (OH) was measured with the laser-induced fluorescence technique (Tan et al., 2017). Volatile organic compounds including methane, C_2-C_{10} hydrocarbons, formaldehyde, and oxygenated hydrocarbons and acetonitrile (CH_3CN) were measured with a cavity ring-down spectroscopy technique instrument, an online gas chromatograph equipped with a mass spectrometer and a flame ionization detector, a Hantzsch fluorimetric monitor, and a proton-transfer-reaction mass spectrometer, respectively (Yuan et al., 2010; Wang et al., 2014). Meteorological data including the wind profile, relative humidity (RH), and temperature were measured with an ultrasonic anemometer and a weather station on a 20m tower. Detailed descriptions of these instrumentation and measurement techniques at Wangdu can be found in previous publications (e.g., Wang Y. et al., 2016; Min et al., 2016; Tham et al., 2016; and Tan et al., 2017).

3 Results and Discussion

3.1 Nocturnal heterogeneous N_2O_5 reaction at Wangdu

Figure 1 illustrates the time series of NO_x, O_3, N_2O_5, $ClNO_2$, particulate NO_3^-, S_a, the calculated production rate of NO_3, and the lifetime of N_2O_5 observed at Wangdu between 20 June and 9 July 2014. The abundance of NO_x and O_3 was observed at night-time (20:00 to 05:00 local time); with average night-time mixing ratios of 21 and 30 ppbv, respectively. The elevated night-time NO_x and O_3 levels led to the active production of NO_3, with an average nighttime production rate of NO_3 ($=k_{O3+NO2}[NO_2][O_3]$) of 1.7 ppb h^{-1} and a maximum level of 8.3 ppb h^{-1} for the entire campaign. Even with the rapid production of NO_3 and the high NO_2 level at night, the observed N_2O_5 concentrations were typically low (i.e., the average nighttime concentration of 34 ± 14 pptv). The low N_2O_5 value is consistent with the short steady-state lifetime of N_2O_5 ($\tau(N_2O_5)$) for the study period, ranged from 0.1 to 10 min, suggesting that the direct loss of N_2O_5 via heterogeneous reaction and/or indirect loss of N_2O_5 via decomposition to NO_3 (i.e., reactions of NO_3 with NO and volatile organic compounds [VOCs]) were rapid in this region. The good correlation between the night-time levels of $ClNO_2$ and fine particulate NO_3^- (the products of heterogeneous reactions of N_2O_5 via R3 and R4, respectively), with a coefficient of determination (r^2) of greater than 0.6 on 10 out of 13 nights (with full CIMS measurement), provides field evidence of active N_2O_5 heterogeneous uptake processes in this region.

3.2 Estimation of N_2O_5 uptake coefficient and $ClNO_2$ production yield

The consistent trends and clear correlation between $ClNO_2$ and the NO_3^- could be used to quantify N_2O_5 heterogeneous uptake following the method described by Phillips et al. (2016). The uptake coefficient of N_2O_5, γ (N_2O_5), was estimated based on the production rate of $ClNO_2$ ($p$$ClNO_2$) and the nitrate formation rate ($p$$NO_3^-$) from the following equation (4). The $p$$ClNO_2$ and $p$$NO_3^-$ were determined from the linear fit of the increase of $ClNO_2$ and total NO_3^- (sum of HNO_3 and particulate NO_3^-) with time, while $[N_2O_5]$ is mean concentration of N_2O_5 for the specified duration.

$$\gamma(N_2O_5)=\frac{2(pClNO_2+pNO_3^-)}{C_{N2O5}S_a[N_2O_5]} \qquad \text{(Eq 4)}$$

The yield of $ClNO_2$ was determined from the regression analysis of $ClNO_2$ versus total NO_3^- (Wagner et al., 2012; Riedel et al., 2013). The slope (m) from the regression plot was fitted into equation (5) to obtain the ϕ.

$$\phi = \frac{2m}{1+m} \qquad \text{(Eq 5)}$$

The concentrations of $ClNO_2$, N_2O_5, total NO_3^-, and other related data used for this analysis were averaged or interpolated into 10 min. This analysis assumes 1) that the air mass is stable, vertical mixing is limited and losses of $ClNO_2$ and total NO_3^- are insignificant within the duration of analysis; and 2) that N_2O_5 heterogeneous uptake is a dominant source of total soluble nitrate during the night rather than the gas homogeneous production or nitrate production from the preceding daytime.

The limitation of this method is that it cannot predict the $\gamma(N_2O_5)$ with negative changes in the concentrations of $ClNO_2$ or total NO_3^-, which may be a result of differences in the origin or age of the air mass. In accordance with this limitation and with the assumption (1) above, we carefully select plumes during the night-time that meet the following criteria for the analysis: shorter periods of data, usually between 1.5 and 4 hours, with concurrent increases in $ClNO_2$ and total NO_3^-. The plume age, represented by the ratios of NO_x to NO_y, was relatively stable (change <0.1 min^{-1}), and no drastic changes were seen in other variables such as wind conditions, the particle surface area, RH, or temperature. Typically, the air masses in the selected cases can be influenced by the emissions from the nearby village/urban area, coal-fired power plants and biomass burning activities in the region prior to the arrival at the site (see Tham et al., 2016). Hence the concentration of NO in the plume must be relatively constant (change of NO/NO_2 ratio <0.1 min^{-1}), as the presence of a transient NO plume may affect the concentration of N_2O_5, which can bias the estimation of $\gamma(N_2O_5)$. Figure 2 shows two examples of relatively constant conditions of relevant chemical composition and environmental variables, together with a plot of $ClNO_2$ versus total NO_3^- for the night. Our previous analysis showed that the nighttime vertical mixing is limited at the ground-site of Wangdu (Tham et al., 2016), and likely will not affect the analysis of $ClNO_2$ and total NO_3^-. It should also be noted that contribution of total NO_3^- from other sources, like the reaction of OH with NO_2 and the oxidation of VOCs by NO_3, can bias the values predicted for $\gamma(N_2O_5)$ and ϕ.

To check the validity of assumptions (2) above, we also calculated the production rate of NO_3^-/HNO_3 via reaction of $OH+NO_2$ ($=k_{OH+NO2}[OH][NO_2]$) and NO_3+VOC ($=\Sigma_i k_i[VOC_i][NO_3]$, where VOC_i = C_2H_6, C_3H_6, C_3H_8, HCHO, CH_3OH, C_2H_4O, $CH_3C(O)CH_3$), as shown in the average diurnal profiles of related species in Figure 3. It is clear that particulate NO_3^- was the dominant species during the night-time at Wangdu, while the nighttime gas-phase HNO_3 is only 7% (on average) of the total NO_3^- (Figure 3b). The strong correlation between $ClNO_2$ and nitrate during the night indicates that the heterogeneous process of N_2O_5 was the dominant source of particulate nitrate. Moreover, the production rate of HNO_3, as calculated from the gas-phase reactions of $OH+NO_2$ and NO_3+VOC, shows a decreasing trend towards the night (Figure 3c), and the combination of these rates on average is less than one-third of the average pNO_3^-, which was determined from the slope of nighttime particulate NO_3^- in Figure 3b. The increase in night-time NO_3^- was also accompanied by an increase in ammonium (NH_4^+), which suggests that the repartition process to form ammonium nitrate was efficient, thus limiting the release of HNO_3 (Figure 3d). These results support the validity of the above assumptions and the determination of uptake and yield in this analysis.

With these methods and selection criteria, we can derive $\gamma(N_2O_5)$ and ϕ for 10 different nighttime plumes in 8 out of 13 nights with full CIMS measurement. Table 1 shows the estimated N_2O_5 uptake coefficients and $ClNO_2$ yields at Wangdu together with the errors that account for the scattering of data in the analysis and uncertainty from the measurement of N_2O_5, $ClNO_2$, aerosol surface area, and total NO_3^-. The estimated $\gamma(N_2O_5)$ values ranged from 0.005 to 0.039, with a mean value of 0.022. A large variability was found in ϕ (range, 0.06 to 1.04). The relatively larger $\gamma(N_2O_5)$ and ϕ values observed on the night of 20–21 June are consistent with the observation of the highest $ClNO_2$ concentration, whereas the lower $\gamma(N_2O_5)$ and ϕ values on the night of 28–29 June explain the observation of the elevated N_2O_5 and small $ClNO_2$ mixing ratios (c.f. Figure 1). The observed $\gamma(N_2O_5)$ and ϕ values at Wangdu were compared with literature values derived from previous field observations in various locations in North America, Europe, and China, as summarized in Figure 4 and Table 2. The variable values of $\gamma(N_2O_5)$ in this study fall in the range of $\gamma(N_2O_5)$ (<0.001 to 0.11) and ϕ (0.01–1.38) reported around the world. The values are also within the range of N_2O_5 uptake coefficients and $ClNO_2$ yields determined in regions of China regions ($\gamma(N_2O_5)$ = 0.004–0.103; ϕ = 0.01–0.98), which are in the middle to upper end of the values reported around the world. The observed significant $ClNO_2$ concentrations and high yields of ϕ here, consistent with other studies at inland sites (c.f. Table 2), also point to the fact that $ClNO_2$ production can be efficient in regions far from the oceanic source of chloride and further highlight the important role of anthropogenic chloride emissions in the chlorine activation process and the next-day's photochemistry. The question that arises here is what drives the large variability in the $\gamma(N_2O_5)$ and ϕ at Wangdu.

3.3 Factors that control the N_2O_5 uptake coefficient

Heterogeneous uptake of N_2O_5 is governed by various factors, including the amount of water and the physical and chemical characteristics of the aerosols (Chang et al., 2011; Brown and Stutz, 2012). To gain better insight into the factors that drive the N_2O_5 heterogeneous uptake, the determined $\gamma(N_2O_5)$ values were compared with those predicted from complex laboratory-derived parameterizations, and their relationships with the aerosol water content and aerosol compositions observed at Wangdu were examined.

The parameterization of N_2O_5 uptake coefficient derived from Bertram and Thornton (2009) ($\gamma_{B\&T}$) assumed a volume-limited reaction of N_2O_5 on mixed aerosols and considered the bulk amount of nitrate, chloride, and water in the aerosol as the controlling factors, which can be expressed by equation (6):

$$\gamma_{B\&T} = Ak\left(1 - \frac{1}{\left(\frac{k_{R3}[\mathrm{H_2O}](\mathrm{l})}{k_{R2b}[\mathrm{NO_3^-}]}\right) + 1 + \left(\frac{k_{R4}[\mathrm{Cl^-}]}{k_{R2b}[\mathrm{NO_3^-}]}\right)}\right) \qquad \text{(Eq 6)}$$

where A is an empirical pre-factor calculated from the volume of aerosol (V), S_a, c_{N2O5}, and Henry's law coefficient of N_2O_5 ($A = 4/c_{N2O5} \times V/S_a \times H_{aq}$); $k = 1.15 \times 10^6 - (1.15 \times 10^6)^{\exp(-0.13[H2O])}$; $k_{R3}/k_{R2b} = 0.06$; and $k_{R4}/k_{R2b} = 29$. The concentration of aerosol liquid water ($[H_2O]$) used in this study was estimated from the E-AIM model IV with inputs of measured bulk aerosol composition of NH_4^+, Na^+, SO_4^{2-}, NO_3^- and Cl^- (http://www.aim.env.uea.ac.uk /aim/model4/model4a.php) (Wexler and Clegg, 2002), and the V/S_a was taken from the field measurement at Wangdu. It should be noted that the parameterization and calculation here assumes an internal mixing of the aerosol chemical species, and the size distribution of $[H_2O]$, $[NO_{3-}]$, and $[Cl^-]$ in aerosols was not considered due to lack of measurement information. The uptake process would vary with size and mixing state of the particles, thus the predicted γ values here may be biased as a result, but represents an average over bulk aerosols. The $\gamma_{B\&T}$ also does not account for the suppression of $\gamma(N_2O_5)$ from the organics, but it is frequently used with the parameterization formulated by Anttila et al. (2006), who treated the organic fraction in the aerosols as a coating, as given in equation (7) (e.g., Morgan et al., 2015; Phillips et al., 2016; Chang et al., 2016). The net uptake of N_2O_5 onto an aqueous core and organic coating ($\gamma_{B\&T+Org}$) can be determined by equation (8).

$$\gamma_{Org} = \frac{4\,RTH_{org}D_{org}R_c}{C_{N2O5}LR_p} \qquad \text{(Eq 7)}$$

$$\frac{1}{\gamma_{B\&T+Org}} = \frac{1}{\gamma_{B\&T}} + \frac{1}{\gamma_{Org}} \qquad \text{(Eq 8)}$$

Here, the H_{org} is the Henry's Law constant of N_2O_5 for organic coating; D_{org} is the solubility and diffusivity of N_2O_5 in the organic coating of thickness L; and R_c and R_p are the radii of the aqueous core and particle, respectively. The particle radius R_p was determined from the measured median radius of the particle surface area distribution. The L was calculated from the volume ratio of the inorganics to total particles volume following the method in Reimer et al. (2009) with the assumption of hydrophobic organic coating (density, 1.27 g cm^{-3}) on the aqueous inorganic core (with a density of 1.77 g cm^{-3}). The aqueous core radius R_c was calculated by subtracting the L from R_p. The $H_{org}D_{org}$ is equal to 0.03 × $H_{aq}D_{aq}$, where H_{aq} = 5000 M atm^{-1} and D_{aq} = 10^{-9} m^2 s^{-1} (Chang et al., 2011 and references therein). In addition, Evan and Jacob (2005) proposed a simpler parameterization of N_2O_5 uptake on sulfate aerosol ($\gamma_{E\&J}$) as a function of temperature and RH, as given by equation (9).

$$\gamma_{E\&J} = (2.79\times10^{-4}+1.3\times10^{-4}\times RH - 3.43\times10^{-6}\times RH^2 + 7.52\times10^{-8}\times RH^3)\times10^{(4\times10^{-2}\times(T-294))} \qquad \text{(Eq 9)}$$

Figure 5 illustrates a comparison of field-derived N_2O_5 uptake coefficients with the values computed from the above parameterizations. The computed $\gamma_{B\&T}$ (red circle) ranged from 0.046 to 0.094 and was consistently higher than the field-derived $\gamma(N_2O_5)$ by up to a factor of 9. By accounting for the effects of organic coating on the N_2O_5 uptake coefficient via equations (7) and (8), the calculated N_2O_5 uptake coefficients (green circle in Figure 5) are significantly underestimated. Note that only six cases were available to compute the $\gamma_{B\&T+Org}$ due to the limited organic aerosols data for the study period. The N_2O_5 uptake coefficients computed from the parameterization suggested by Evan and Jacob (2005) are generally consistent with the field-derived $\gamma(N_2O_5)$ (as shown by blue circles). The different results from these parameterizations may suggest more complex aerosol composition, mixing states and other physical-chemical properties in the real ambient atmosphere than in the aerosol sample used in the laboratory study.

We then examine the relationships of the field-derived $\gamma(N_2O_5)$ with RH, water content, and aerosol compositions, as illustrated in Figure 6. It can be seen in Figure 6a that the $\gamma(N_2O_5)$ has a clear correlation with the aerosol water content (r^2 = 0.88; $p < 0.01$, t-test). The strong dependence of $\gamma(N_2O_5)$ on the aerosol water content was observed at RH lower than 80% or $[H_2O]$ lower than 40 mol L^{-1}. The $\gamma(N_2O_5)$ then plateaus at about 0.035 when the RH exceeds 80%. This pattern is similar to the trends observed in laboratory studies for N_2O_5 uptake onto aqueous sulfate and malonic acid aerosols, in which the $\gamma(N_2O_5)$ strongly increases with humidity at RH below 40-50% but becomes insensitive above this threshold (e.g., Hallquist et al., 2003; Thornton et al., 2003). The $\gamma(N_2O_5)$ at Wangdu shows a trend of decreasing with the concentration of NO_3^- per volume of aerosol (see Figure 5b), which is similar to the results from the previous laboratory studies (Bertram and Thornton, 2009; Griffiths et al., 2009). However, we do not think that $[NO_3^-]$ is the dominant limiting factor for N_2O_5 uptake at this site, as seen in the consistency of the $\gamma(N_2O_5)$ data points with the change in RH (in the color code of Figure 6b), the increasing trend of $\gamma(N_2O_5)$ with the concentration of particulate nitrate in the air (c.f. Figure 6c), and the positive dependency of $\gamma(N_2O_5)$ on the molar ratio of $[H_2O]/[NO_3^-]$ (c.f. Figure 6d), which reflect that the N_2O_5 uptake is more sensitive to the aerosol water content than to the NO_3^-, at least up to $[H_2O]:[NO_3^-]$ of 20. The increase in ambient particulate nitrate is probably due to the faster N_2O_5 heterogeneous reaction. The N_2O_5 uptake does not show an increasing trend with the chloride-to-nitrate molar ratio, a pattern demonstrated in the laboratory result (Bertram and Thornton, 2009), but rather a decrease for high $[Cl^-]/[NO_3^-]$ ratios, and it also correlates with differences in RH (c.f. Figure 6e). There is a lack of correlation of $\gamma(N_2O_5)$ with the $[Org]:[SO_4^{2-}]$ observed in the ratio range of 0.5–1.2, indicating that the suppression of organics on the N_2O_5 uptake may be insignificant at Wangdu. These results are in line with the parameterization comparison results shown in Figure 5, reveal that the variation in the N_2O_5 uptake at Wangdu is not driven by the chemical properties of aerosols like NO_3^-, Cl^-, and organics, but rather that the

RH or the aerosol water content plays a defining role in the N_2O_5 heterogeneous uptake.

The response of N_2O_5 uptake to the changes in RH is consistent with the changes in the sulfate (SO_4^{2-}) concentrations (see Figure 6g), which mainly determine the hygroscopicity of the aerosols and were found to be responsible for the particle growth at Wangdu (Wu et al., 2017). The hygroscopic growth of aerosols inferred by the RH (water uptake) can affect the amount of water in the aerosol and the volume-to-surface area ratio ($[H_2O]V/S_a$). The good positive correlation of $\gamma(N_2O_5)$ with $[H_2O]V/S_a$ (see Figure 6h) suggests that the increased volume of aerosol, in particular the layer of aerosol water content, could allow efficient diffusion of N_2O_5 and solvation of N_2O_5 into $H_2ONO_2^+$ and NO_3^- for further aqueous reactions, whereas a smaller volume of aerosol (less water content) may be easily saturated by N_2O_5 and then diffuse the N_2O_5 out of the aerosol, limiting the solvation of the N_2O_5 process and restricting N_2O_5 uptake. These results are consistent with several laboratory studies which have demonstrated that an increase in RH enhanced the particle aqueous volume and increased the bulk reactive N_2O_5 uptake on aqueous sulfate and organic acids (e.g., malonic, succinic, and glutaric acid) containing aerosols (Thornton et al., 2003; Hallquist et al., 2003). The increase in RH can also lower the viscosity of the aqueous layer in organic-containing aerosols, leading to greater diffusivity of N_2O_5 within the aerosol water layer, which ultimately increases the N_2O_5 uptake (Gržinic et al., 2015).

The strong dependency of N_2O_5 uptake upon the RH has not been clearly demonstrated in other field measurements. Field observations of $\gamma(N_2O_5)$ in North America and Europe show any significant direct dependence of $\gamma(N_2O_5)$ on RH but were strongly influenced by the aerosol composition (refer to the descriptions in Table 2). For instance, the flight measurements in Texas and London showed the independence of $\gamma(N_2O_5)$ at RH from 34% to 90%, but the $\gamma(N_2O_5)$ were generally controlled by the amount of NO_3^- and/or organic compounds (Brown et al., 2009; Morgan et al., 2015). A comparison of ground measurements in Seattle and Boulder showed variations in $\gamma(N_2O_5)$ at various $H_2O(l)$ levels in the two places, but the RH alone was insufficient to describe their observed $\gamma(N_2O_5)$ variability, and the organic composition of the aerosols was determined to have a dominant influences on $\gamma(N_2O_5)$ (Bertram et al., 2009). Another study from a mountainous site in Germany reported no significant correlation of $\gamma(N_2O_5)$ with aerosol compositions and only a weak dependence on humidity (Phillips et al., 2016). However, field measurements at Jinan and Mt. Tai in northern China during the same season also showed a positive relationship of $\gamma(N_2O_5)$ with an RH between 43% and 72% and aerosol water content of 31–65 mol L^{-1}, respectively (Wang X. et al., 2017; Wang Z. et al., 2017). The results of this study and previously reported results in the region may suggest that RH and aerosol water content are the important limiting factors for the N_2O_5 heterogeneous process in polluted northern China. In summary, the more complex parameterizations considering nitrate, chloride, and the organic coating cannot fully represent the variation of $\gamma(N_2O_5)$ at Wangdu; instead, a simple parameterization that accounts only for temperature and RH appears to explain the variation in $\gamma(N_2O_5)$ at Wangdu. It would be of great interest to determine whether such a phenomenon can be found in other places.

3.4 Factors that affect the $ClNO_2$ production yield

In addition to the uptake coefficients, the factors that influence the branching yield of $ClNO_2$ from the N_2O_5 heterogeneous uptake were also assessed. Figure 7a shows the scatter plot of the ϕ calculated from equation (3) versus the $ClNO_2$ yield derived from the Wangdu field data from equation (5) in Section 3.2. Generally, the $\phi_{param.}$ shows less variability but was obviously overestimated relative to the field-determined ϕ. Such a discrepancy has also been observed elsewhere (Thonton et al., 2010; Mielke et al., 2013; Riedel et al., 2013), including our recent observations in an urban site (Jinan) and a mountaintop site (Mt. Tai) in northern China, where the parameterized ϕ would be overestimated by up to two orders of magnitude (Wang X. et al., 2017; Wang Z. et al., 2017). Further analysis by linking the field-derived $ClNO_2$ yields with the aerosol water content (Figure 7b) and the Cl^- content (Figure 7c) show a weak positive correlation ($r^2 = 0.36$) and a weak negative trend ($r^2 = 0.20$), respectively (from quadratic fitting). The weak correlations reflect that the $ClNO_2$ yield is not solely controlled by the amount of water and chloride in the aerosol, as defined in the parameterization (see Eq. 3), and/or the existence of other nucleophiles that can compete with Cl^- in reactions R3 and R4. The aqueous concentration of Cl^- in the present study is relatively higher than previous laboratory studies (e.g., Bertram and Thornton, 2009; Roberts et al., 2009), and might not be fully involved in the reaction R4, for example, the possible effect of the nonuniform distribution of chloride within the aerosol. It might contribute to the overestimation and less variability of ϕ predicted from the parameterization (Riedel et al., 2013) and the positive relationship of field-derived ϕ with $[H_2O]$ (see Figure 7b) might also imply that the increase of water content could increase the availability of the aerosol Cl^-, thus prompting the reaction R4 to increase the $ClNO_2$ production yield.

An interesting observation from Wangdu is that the field-derived ϕ shows a decreasing trend ($r^2 = 0.58$ from quadratic data fitting) with the ratio of acetonitrile to carbon monoxide (CH_3CN/CO), which is an indicator of biomass burning emission (Christian et al., 2003; Akagi et al., 2011), as illustrated in Figure 7d. The ϕ decreased at larger CH_3CN/CO ratios, which corresponds to higher $[Cl^-]$ concentrations per volume of aerosols (c.f. Figure 7c) because biomass burning emits a significant level of chloride particles. The observations here may suggest that the ϕ is likely “suppressed” in air masses influenced by biomass burning, which were frequently observed during the study period (Tham et al., 2016), and is consistent with the recent field observation of much lower concentrations of $ClNO_2$ during the bonfire event in Manchester compared to that after the event (Reyes-Villegas et al., 2017) and with a laboratory experiment which demonstrated that only a small amount (~10%) of reacted N_2O_5 was converted to $ClNO_2$ on the biomass-burning aerosols (Ahern et al., 2017). Another laboratory study showed that the $ClNO_2$ yield can be reduced by as much as 80% in the presence of aromatic organic compounds like phenol and humic acid in the aerosol (Ryder et al., 2015), and previous studies in China reported abundant humic-like substances (e.g., aromatic organic compounds) in aerosols with a large contribution from biomass burning (Fu et al., 2008). Therefore, the frequently observed influence of biomass burning at the Wangdu site during the campaign could in part explain the lower ϕ values and the discrepancy between observation and parameterization. More studies are needed to investigate the effects of biomass burning emissions on the heterogeneous process.

4 Summary and conclusions

We present an in-depth analysis of the N_2O_5 uptake coefficient and $ClNO_2$ yield in a polluted northern China environment during the summer of 2014. Large variations in the levels of $\gamma(N_2O_5)$ and ϕ were observed during the study, ranging from 0.005 to 0.039 and from 0.06 to 1.04, respectively. A comparison between the $\gamma(N_2O_5)$ values derived from the field and the parameterizations that considered the nitrate and chloride levels and the hydrophobic organic coating showed poor agreement, suggesting more complex influences of ambient aerosol properties at the site than with the pure or mixed samples used in the laboratory. The $\gamma(N_2O_5)$ values at Wangdu were found to have a clear dependence on the RH and the aerosol water content, a phenomenon that was found in laboratory experiments but has not been observed in previous field studies in the United States or Europe. The parameterization that explicitly considers the dependence on RH showed better agreement with the field-derived $\gamma(N_2O_5)$ compared to the more complex formulation that considers the aerosol composition. The $ClNO_2$ yield estimated from the parameterization is generally overestimated when compared to the field derived values. The observed ϕ was found to be "suppressed" in the air masses influenced by biomass burning even though abundant aerosol chloride was present. The results of this study point to the need for more field and laboratory studies to obtain realistic parameterization of the heterogeneous processes of N_2O_5 and $ClNO_2$ to better simulate the ozone and aerosol production in air quality models in regions of China with high NO_x emissions.

Acknowledgment. The authors thank Steven Poon, Qiaozhi Zha, Zheng Xu and Hao Wang for the logistics support, to Liming Cao and Lingyan He for providing the aerosol mass spectrometer data and to Li Zhang for scientific discussion. This work was funded by the National Natural Science Foundation of China (91544213, 41505103 and 41275123), National Key Research and Development Program of China (2016YFC0200500), Research Grants Council of Hong Kong (15265516), PolyU Project of Strategic Importance (1-ZE13) and Research Institute for Sustainable Urban Development (RISUD). The Peking University team acknowledges support from the National Natural Science Foundation of China (21190052) and the Strategic Priority Research Program of the Chinese Academy of Sciences (XDB05010500). The Leibniz Institute for Tropospheric Research team acknowledges funding from the Sino German Science Center (No. GZ663).

References

Ahern, A., Goldberger, L., Jahl, L., Thornton, J., and Sullivan, R. C.: Production of N_2O_5 and $ClNO_2$ through nocturnal processing of biomass-burning aerosol, Environ. Sci. Technol., 10.1021/acs.est.7b04386, 2017.

Akagi, S. K., Yokelson, R. J., Wiedinmyer, C., Alvarado, M. J., Reid, J. S., Karl, T., Crounse, J. D., and Wennberg, P. O.: Emission factors for open and domestic biomass burning for use in atmospheric models, Atmos. Chem. Phys., 11, 4039-4072, 10.5194/acp-11-4039-2011, 2011.

Anttila, T., Kiendler-Scharr, A., Tillmann, R., and Mentel, T. F.: On the reactive uptake of gaseous compounds by organic-coated aqueous aerosols: theoretical analysis and application to the heterogeneous hydrolysis of N_2O_5, J. Phys. Chem. A, 110, 10435-10443, 10.1021/jp062403c, 2006.

Behnke, W., George, C., Scheer, V., and Zetzsch, C.: Production and decay of $ClNO_2$, from the reaction of gaseous N_2O_5 with NaCl solution: Bulk and aerosol experiments, J. Geophys. Res.-Atmos., 102, 3795-3804, Doi 10.1029/96jd03057, 1997.

Bertram, T. H., and Thornton, J. A.: Toward a general parameterization of N_2O_5 reactivity on aqueous particles: the competing effects of particle liquid water, nitrate and chloride, Atmos. Chem. Phys., 9, 8351-8363, 10.5194/acp-9-8351-2009, 2009.

Bertram, T. H., Thornton, J. A., Riedel, T. P., Middlebrook, A. M., Bahreini, R., Bates, T. S., Quinn, P. K., and Coffman, D. J.: Direct observations of N_2O_5 reactivity on ambient aerosol particles, Geophys. Res. Lett., 36, L19803, 10.1029/2009gl040248, 2009.

Brown, S. S., and Stutz, J.: Nighttime radical observations and chemistry, Chem. Soc. Rev., 41, 6405-6447, 2012.

Brown, S. S., Dube, W. P., Fuchs, H., Ryerson, T. B., Wollny, A. G., Brock, C. A., Bahreini, R., Middlebrook, A. M., Neuman, J. A., Atlas, E., Roberts, J. M., Osthoff, H. D., Trainer, M., Fehsenfeld, F. C., and Ravishankara, A. R.: Reactive uptake coefficients for N_2O_5 determined from aircraft measurements during the Second Texas Air Quality Study: Comparison to current model parameterizations, J. Geophys. Res.-Atmos., 114, D00F10, 10.1029/2008jd011679, 2009.

Brown, S. S., Dube, W. P., Tham, Y. J., Zha, Q. Z., Xue, L. K., Poon, S., Wang, Z., Blake, D. R., Tsui, W., Parrish, D. D., and Wang, T.: Nighttime chemistry at a high altitude site above Hong Kong, J. Geophys. Res.-Atmos., 121, 2457-2475, 10.1002/2015JD024566, 2016.

Brown, S., Ryerson, T., Wollny, A., Brock, C., Peltier, R., Sullivan, A., Weber, R., Dube, W., Trainer, M., Meagher, J. Fehsenfeld, F. C., and Ravishankara, A. R.: Variability in nocturnal nitrogen oxide processing and its role in regional air quality, Science, 311, 67-70, 2006.

Chang, W. L., Bhave, P. V., Brown, S. S., Riemer, N., Stutz, J., and Dabdub, D.: Heterogeneous atmospheric chemistry, ambient measurements, and model calculations of N_2O_5: A review, Aerosol Sci. Tech., 45, 665-695, 10.1080/02786826.2010.551672, 2011.

Chang, W. L., Brown, S. S., Stutz, J., Middlebrook, A. M., Bahreini, R., Wagner, N. L., Dube, W. P., Pollack, I. B., Ryerson, T. B., and Riemer, N.: Evaluating N_2O_5 heterogeneous hydrolysis parameterizations for CalNex 2010, J. Geophys. Res.-Atmos., 121, 5051-5070, 10.1002/2015JD024737, 2016.

Christian, T. J., Kleiss, B., Yokelson, R. J., Holzinger, R., Crutzen, P. J., Hao, W. M., Saharjo, B. H., and Ward, D. E.: Comprehensive laboratory measurements of biomass-burning emissions: 1. Emissions from Indonesian, African, and other fuels, J. Geophys. Res.-Atmos., 108, 10.1029/2003JD003704, 2003.

Cosman, L. M., Knopf, D. A., and Bertram, A. K.: N_2O_5 reactive uptake on aqueous sulfuric acid solutions coated with branched and straight-chain insoluble organic surfactants, J. Phys. Chem. A, 112, 2386–2396, doi:10.1021/jp710685r, 2008.

Davis, J., Bhave, P., and Foley, K.: Parameterization of N_2O_5 reaction probabilities on the surface of particles containing ammonium, sulfate, and nitrate, Atmos. Chem. Phys., 8, 5295-5311, 2008.

Dong, H. B., Zeng, L. M., Hu, M., Wu, Y. S., Zhang, Y. H., Slanina, J., Zheng, M., Wang, Z. F., and Jansen, R.: Technical Note: The application of an improved gas and aerosol collector for ambient air pollutants in China, Atmos. Chem. Phys., 12, 10519-10533, 10.5194/acp-12-10519-2012, 2012.

Evans, M. J., and Jacob, D. J.: Impact of new laboratory studies of N_2O_5 hydrolysis on global model budgets of tropospheric nitrogen oxides, ozone, and OH, Geophys. Res. Lett., 32, 10.1029/2005gl022469, 2005.

Finlayson-Pitts, B., Ezell, M., and Pitts, J.: Formation of chemically active chlorine compounds by reactions of atmospheric NaCl particles with gaseous N_2O_5 and $ClONO_2$, Nature, 337, 241-244, 1989.

Folkers, M., Mentel, T. F., and Wahner, A.: Influence of an organic coating on the reactivity of aqueous aerosols probed by the heterogeneous hydrolysis of N_2O_5, Geophys. Res. Lett., 30, 2003.

Fu, P., Kawamura, K., Okuzawa, K., Aggarwal, S. G., Wang, G., Kanaya, Y., and Wang, Z.: Organic molecular compositions and temporal variations of summertime mountain aerosols over Mt. Tai, North China Plain, J. Geophys. Res.-Atmos., 113, 10.1029/2008JD009900, 2008.

Fuchs, H., Tan, Z., Lu, K., Bohn, B., Broch, S., Brown, S. S., Dong, H., Gomm, S., Häseler, R., He, L., Hofzumahaus, A., Holland, F., Li, X., Liu, Y., Lu, S., Min, K. E., Rohrer, F., Shao, M., Wang, B., Wang, M., Wu, Y., Zeng, L., Zhang, Y., Wahner, A., and Zhang, Y.: OH reactivity at a rural site (Wangdu) in the North China Plain: contributions from OH reactants and experimental OH budget, Atmos. Chem. Phys., 17, 645-661, 10.5194/acp-17-645-2017, 2017.

Gaston, C. J., and Thornton, J. A.: Reacto-diffusive length of N_2O_5 in aqueous sulfate-and chloride-containing aerosol particles, J. Phys. Chem. A, 120, 1039-1045, 2016.

Gaston, C. J., Thornton, J. A., and Ng, N. L.: Reactive uptake of N_2O_5 to internally mixed inorganic and organic particles: the role of organic carbon oxidation state and inferred organic phase separations, Atmos. Chem. Phys., 14, 5693-5707, 10.5194/acp-14-5693-2014, 2014.

Griffiths, P. T., Badger, C. L., Cox, R. A., Folkers, M., Henk, H. H., and Mentel, T. F.: Reactive uptake of N_2O_5 by aerosols containing dicarboxylic acids. Effect of particle phase, composition, and nitrate content, J. Phys. Chem. A, 113, 5082-5090, 10.1021/jp8096814, 2009.

Gržinić, G., Bartels-Rausch, T., Berkemeier, T., Türler, A., and Ammann, M.: Viscosity controls humidity dependence of N_2O_5 uptake to citric acid aerosol, Atmos. Chem. Phys., 15, 13615-13625, 2015.

Hallquist, M., Stewart, D. J., Stephenson, S. K., and Cox, R. A.: Hydrolysis of N_2O_5 on sub-micron sulfate aerosols, Phys. Chem. Chem. Phys., 5, 3453-3463, 2003.

Hennig, T., Massling, A., Brechtel, F. J., and Wiedensohler, A.: A tandem DMA for highly temperature-stabilized hygroscopic particle growth measurements between 90% and 98% relative humidity, J. Aerosol Sci., 36, 1210-1223, 10.1016/j.jaerosci.2005.01.005, 2005.

Kercher, J. P., Riedel, T. P., and Thornton, J. A.: Chlorine activation by N_2O_5: simultaneous, in situ detection of $ClNO_2$ and N_2O_5 by chemical ionization mass spectrometry, Atmos. Meas. Tech., 2, 193-204, 10.5194/amt-2-193-2009, 2009.

Kuang, B. Y., Lin, P., Huang, X. H. H., and Yu, J. Z.: Sources of humic-like substances in the Pearl River Delta, China: positive matrix factorization analysis of $PM_{2.5}$ major components and source markers, Atmos. Chem. Phys., 15, 1995-2008, 10.5194/acp-15-1995-2015, 2015.

Kuang, Y., Zhao, C., Ma, N., Liu, H., Bian, Y., Tao, J., and Hu, M.: Deliquescent phenomena of ambient aerosols on the North China Plain, Geophys. Res. Lett., 43, 8744-8750, 2016.

Li, Q., Zhang, L., Wang, T., Tham, Y.J., Ahmadov, R., Xue, L., Zhang, Q., Zheng, J.: Impacts of heterogeneous uptake of dinitrogen pentoxide and chlorine activation on ozone and reactive nitrogen partitioning: improvement and application of the WRF-Chem model in southern China. Atmos. Chem. Phys., 16, 14875-14890, 2016.

Lin, P., Engling, G., and Yu, J. Z.: Humic-like substances in fresh emissions of rice straw burning and in ambient aerosols in the Pearl River Delta Region, China, Atmos. Chem. Phys., 10, 6487-6500, 10.5194/acp-10-6487-2010, 2010.

Liu, H. J., Zhao, C. S., Nekat, B., Ma, N., Wiedensohler, A., van Pinxteren, D., Spindler, G., Muller, K., and Herrmann, H.: Aerosol hygroscopicity derived from size-segregated chemical composition and its parameterization in the North China Plain, Atmos. Chem. Phys., 14, 2525-2539, 10.5194/acp-14-2525-2014, 2014.

Liu, X., Qu, H., Huey, L. G., Wang, Y., Sjostedt, S., Zeng, L., Lu, K., Wu, Y., Hu, M., Shao, M., Zhu, T., and Zhang, Y.: High levels of daytime molecular chlorine and nitryl chloride at a rural site on the North China Plain, Environ. Sci. Technol., 51, 9588-9595, 10.1021/acs.est.7b03039, 2017.

McDuffie, E. E., Fibiger, D. L., Dubé, W. P., Lopez-Hilfiker, F., Lee, B. H., Thornton, J. A., Shah, V., Jaeglé, L., Guo, H., Weber, R. J., Michael Reeves, J., Weinheimer, A. J., Schroder, J. C., Campuzano-Jost, P., Jimenez, J. L., Dibb, J. E., Veres, P., Ebben, C., Sparks, T. L., Wooldridge, P. J., Cohen, R. C., Hornbrook, R. S., Apel, E. C., Campos, T., Hall, S. R., Ullmann, K., and Brown, S. S.: Heterogeneous N2O5 Uptake During Winter: Aircraft Measurements During the 2015 WINTER Campaign and Critical Evaluation of Current Parameterizations, J. Geophys. Res.-Atmos., 123, 4345-4372, doi:10.1002/2018JD028336, 2018.

Mentel, T. F., Sohn, M., and Wahner, A.: Nitrate effect in the heterogeneous hydrolysis of dinitrogen pentoxide on aqueous aerosols, Phys. Chem. Chem. Phys., 1, 5451-5457, Doi 10.1039/A905338g, 1999.

Mielke, L. H., Furgeson, A., and Osthoff, H. D.: Observation of $ClNO_2$ in a mid-continental urban environment, Environ. Sci. Technol., 45, 8889-8896, 10.1021/es201955u, 2011.

Mielke, L. H., Stutz, J., Tsai, C., Hurlock, S. C., Roberts, J. M., Veres, P. R., Froyd, K. D., Hayes, P. L., Cubison, M. J., Jimenez, J. L., Washenfelder, R. A., Young, C. J., Gilman, J. B., de Gouw, J. A., Flynn, J. H., Grossberg, N., Lefer, B. L., Liu, J., Weber, R. J., and Osthoff, H. D.: Heterogeneous formation of nitryl chloride and its role as a nocturnal NOx reservoir species during CalNex-LA 2010, J. Geophys. Res.-Atmos., 118, 10638-10652, 10.1002/jgrd.50783, 2013.

Min, K. E., Washenfelder, R. A., Dubé, W. P., Langford, A. O., Edwards, P. M., Zarzana, K. J., Stutz, J., Lu, K., Rohrer, F., Zhang, Y., and Brown, S. S.: A broadband cavity enhanced absorption spectrometer for aircraft measurements of glyoxal, methylglyoxal, nitrous acid, nitrogen dioxide, and water vapor, Atmos. Meas. Tech., 9, 423-440, 10.5194/amt-9-423-2016, 2016.

Morgan, W. T., Ouyang, B., Allan, J. D., Aruffo, E., Di Carlo, P., Kennedy, O. J., Lowe, D., Flynn, M. J., Rosenberg, P. D., Williams, P. I., Jones, R., McFiggans, G. B., and Coe, H.: Influence of aerosol chemical composition on N_2O_5 uptake: airborne regional measurements in northwestern Europe, Atmos. Chem. Phys., 15, 973-990, 10.5194/acp-15-973-2015, 2015.

Nie, W., Hong, J., Häme, S. A. K., Ding, A., Li, Y., Yan, C., Hao, L., Mikkilä, J., Zheng, L., Xie, Y., Zhu, C., Xu, Z., Chi, X., Huang, X., Zhou, Y., Lin, P., Virtanen, A., Worsnop, D. R., Kulmala, M., Ehn, M., Yu, J., Kerminen, V. M., and Petäjä, T.: Volatility of mixed atmospheric humic-like substances and ammonium sulfate particles, Atmos. Chem. Phys., 17, 3659-3672, 10.5194/acp-17-3659-2017, 2017.

Osthoff, H. D., Roberts, J. M., Ravishankara, A. R., Williams, E. J., Lerner, B. M., Sommariva, R., Bates, T. S., Coffman, D., Quinn, P. K., Dibb, J. E., Stark, H., Burkholder, J. B., Talukdar, R. K., Meagher, J., Fehsenfeld, F. C., and Brown, S. S.: High levels of nitryl chloride in the polluted subtropical marine boundary layer, Nature Geosci, 1, 324-328, 2008.

Pathak, R. K., Wang, T., and Wu, W. S.: Nighttime enhancement of $PM_{2.5}$ nitrate in ammonia-poor atmospheric conditions in Beijing and Shanghai: Plausible contributions of heterogeneous hydrolysis of N_2O_5 and HNO_3 partitioning, Atmos. Environ., 45, 1183-1191, https://doi.org/10.1016/j.atmosenv.2010.09.003, 2011.

Pathak, R. K., Wu, W. S., and Wang, T.: Summertime $PM_{2.5}$ ionic species in four major cities of China: nitrate formation in an ammonia-deficient atmosphere, Atmos. Chem. Phys., 9, 1711-1722, 10.5194/acp-9-1711-2009, 2009.

Phillips, G. J., Thieser, J., Tang, M., Sobanski, N., Schuster, G., Fachinger, J., Drewnick, F., Borrmann, S., Bingemer, H., Lelieveld, J., and Crowley, J. N.: Estimating N_2O_5 uptake coefficients using ambient measurements of NO_3, N_2O_5, $ClNO_2$ and particle-phase nitrate, Atmos. Chem. Phys., 16, 13231-13249, 10.5194/acp-16-13231-2016, 2016.

Reyes-Villegas, E., Priestley, M., Ting, Y. C., Haslett, S., Bannan, T., Le breton, M., Williams, P. I., Bacak, A., Flynn, M. J., Coe, H., Percival, C., and Allan, J. D.: Simultaneous Aerosol Mass Spectrometry and Chemical Ionisation Mass Spectrometry measurements during a biomass burning event in the UK: Insights into nitrate chemistry, Atmos. Chem. Phys. Discuss., 2017, 1-22, 10.5194/acp-2017-605, 2017.

Riedel, T. P., Bertram, T. H., Crisp, T. A., Williams, E. J., Lerner, B. M., Vlasenko, A., Li, S.-M., Gilman, J., de Gouw, J., Bon, D. M., Wagner, N. L., Brown, S. S., and Thornton, J. A.: Nitryl chloride and molecular chlorine in the coastal marine boundary layer, Environ. Sci. Technol., 46, 10463-10470, 10.1021/es204632r, 2012a.

Riedel, T. P., Bertram, T. H., Ryder, O. S., Liu, S., Day, D. A., Russell, L. M., Gaston, C. J., Prather, K. A., and Thornton, J. A.: Direct N_2O_5 reactivity measurements at a polluted coastal site, Atmos. Chem. Phys., 12, 2959-2968, 10.5194/acp-12-2959-2012, 2012b.

Riedel, T. P., Wagner, N. L., Dube, W. P., Middlebrook, A. M., Young, C. J., Ozturk, F., Bahreini, R., VandenBoer, T. C., Wolfe, D. E., Williams, E. J., Roberts, J. M., Brown, S. S., and Thornton, J. A.: Chlorine activation within urban or power plant plumes: Vertically resolved $ClNO_2$ and Cl_2 measurements from a tall tower in a polluted continental setting, J. Geophys. Res.-Atmos., 118, 8702-8715, 10.1002/jgrd.50637, 2013.

Riedel, T. P., Wolfe, G. M., Danas, K. T., Gilman, J. B., Kuster, W. C., Bon, D. M., Vlasenko, A., Li, S. M., Williams, E. J., Lerner, B. M., Veres, P. R., Roberts, J. M., Holloway, J. S., Lefer, B., Brown, S. S., and Thornton, J. A.: An MCM modeling study of nitryl chloride ($ClNO_2$) impacts on oxidation, ozone production and nitrogen oxide partitioning in polluted continental outflow, Atmos. Chem. Phys., 14, 3789-2014, 2014.

Riemer, N., Vogel, H., Vogel, B., Anttila, T., Kiendler‐Scharr, A., and Mentel, T.: Relative importance of organic coatings for the heterogeneous hydrolysis of N_2O_5 during summer in Europe, J. Geophys. Res.-Atmos., 114, 2009.

Roberts, J. M., Osthoff, H. D., Brown, S. S., Ravishankara, A. R., Coffman, D., Quinn, P., and Bates, T.: Laboratory studies of products of N_2O_5 uptake on Cl^- containing substrates, Geophys. Res. Lett., 36, L20808, 10.1029/2009GL040448, 2009.

Ryder, O. S., Ault, A. P., Cahill, J. F., Guasco, T. L., Riedel, T. P., Cuadra-Rodriguez, L. A., Gaston, C. J., Fitzgerald, E., Lee, C., Prather, K. A., and Bertram, T. H.: On the role of particle inorganic mixing state in the reactive uptake of N2O5 to ambient aerosol particles, Environ. Sci. Technol., 48, 1618-1627, 10.1021/es4042622, 2014.

Ryder, O. S., Campbell, N. R., Shaloski, M., Al-Mashat, H., Nathanson, G. M., and Bertram, T. H.: Role of Organics in Regulating $ClNO_2$ Production at the Air-Sea Interface, J. Phys. Chem. A, 119, 8519-8526, 10.1021/jp5129673, 2015.

Sarwar, G., Simon, H., Xing, J., and Mathur, R.: Importance of tropospheric $ClNO_2$ chemistry across the Northern Hemisphere, Geophys. Res. Lett., 41, 2014GL059962, 10.1002/2014GL059962, 2014.

Schweitzer, F., Mirabel, P., and George, C.: Multiphase chemistry of N_2O_5, $ClNO_2$, and $BrNO_2$, J. Phys. Chem. A, 102, 3942-3952, Doi 10.1021/Jp980748s, 1998.

Tan, Z., Fuchs, H., Lu, K., Hofzumahaus, A., Bohn, B., Broch, S., Dong, H., Gomm, S., Häseler, R., He, L., Holland, F., Li, X., Liu, Y., Lu, S., Rohrer, F., Shao, M., Wang, B., Wang, M., Wu, Y., Zeng, L., Zhang, Y., Wahner, A., and Zhang, Y.: Radical chemistry at a rural site (Wangdu) in the North China Plain: observation and model calculations of OH, HO_2 and RO_2 radicals, Atmos. Chem. Phys., 17, 663-690, 10.5194/acp-17-663-2017, 2017.

Tang, M. J., Telford, P. J., Pope, F. D., Rkiouak, L., Abraham, N. L., Archibald, A. T., Braesicke, P., Pyle, J. A., McGregor, J., Watson, I. M., Cox, R. A., and Kalberer, M.: Heterogeneous reaction of N2O5 with airborne TiO2 particles and its implication for stratospheric particle injection, Atmos. Chem. Phys., 14, 6035-6048, 2014.

Tang, M., Huang, X., Lu, K., Ge, M., Li, Y., Cheng, P., Zhu, T., Ding, A., Zhang, Y., Gligorovski, S., Song, W., Ding, X., Bi, X., and Wang, X.: Heterogeneous reactions of mineral dust aerosol: implications for tropospheric oxidation capacity, Atmos. Chem. Phys., 17, 11727-11777, 10.5194/acp-17-11727-2017, 2017.

Tham, Y. J., Wang, Z., Li, Q., Yun, H., Wang, W., Wang, X., Xue, L., Lu, K., Ma, N., Bohn, B., Li, X., Kecorius, S., Größ, J., Shao, M., Wiedensohler, A., Zhang, Y., and Wang, T.: Significant concentrations of nitryl chloride sustained in the morning: investigations of the causes and impacts on ozone production in a polluted region of northern China, Atmos. Chem. Phys., 16, 14959-14977, 10.5194/acp-16-14959-2016, 2016.

Tham, Y. J., Yan, C., Xue, L., Zha, Q., Wang, X., and Wang, T.: Presence of high nitryl chloride in Asian coastal environment and its impact on atmospheric photochemistry, Chin. Sci. Bull., 59, 356-359, 10.1007/s11434-013-0063-y, 2014.

Thornton, J. A., and Abbatt, J. P. D.: N_2O_5 reaction on submicron sea salt aerosol: Kinetics, products, and the effect of surface active organics, J. Phys. Chem. A, 109, 10004-10012, 10.1021/jp054183t, 2005.

Thornton, J. A., Braban, C. F., and Abbatt, J. P.: N_2O_5 hydrolysis on sub-micron organic aerosols: The effect of relative humidity, particle phase, and particle size, Phys. Chem. Chem. Phys., 5, 4593-4603, 2003.

Thornton, J. A., Kercher, J. P., Riedel, T. P., Wagner, N. L., Cozic, J., Holloway, J. S., Dubé, W. P., Wolfe, G. M., Quinn, P. K., Middlebrook, A. M., Alexander, B., and Brown, S. S.: A large atomic chlorine source inferred from mid-continental reactive nitrogen chemistry, Nature, 464, 271-274, 2010.

Wagner, N. L., Riedel, T. P., Roberts, J. M., Thornton, J. A., Angevine, W. M., Williams, E. J., Lerner, B. M., Vlasenko, A., Li, S. M., Dube, W. P., Coffman, D. J., Bon, D. M., de Gouw, J. A., Kuster, W. C., Gilman, J. B., and Brown, S. S.: The sea breeze/land breeze circulation in Los Angeles and its influence on nitryl chloride production in this region, J. Geophys. Res.-Atmos., 117, D00V24, 10.1029/2012jd017810, 2012.

Wagner, N. L., Riedel, T. P., Young, C. J., Bahreini, R., Brock, C. A., Dubé, W. P., Kim, S., Middlebrook, A. M., Öztürk, F., Roberts, J. M., Russo, R., Sive, B., Swarthout, R., Thornton, J. A., VandenBoer, T. C., Zhou, Y., and Brown, S. S.: N_2O_5 uptake coefficients and nocturnal NO_2 removal rates determined from ambient wintertime measurements, J. Geophys. Res.-Atmos., 118, 9331-9350, 10.1002/jgrd.50653, 2013.

Wang, H., Lu, K., Chen, X., Zhu, Q., Chen, Q., Guo, S., Jiang, M., Li, X., Shang, D., Tan, Z., Wu, Y., Wu, Z., Zou, Q., Zheng, Y., Zeng, L., Zhu, T., Hu, M., and Zhang, Y.: High N_2O_5 Concentrations Observed in Urban Beijing: Implications of a Large Nitrate Formation Pathway, Environ. Sci. Technol. Lett., 4, 416-420, 10.1021/acs.estlett.7b00341, 2017.

Wang, H., Lu, K., Guo, S., Wu, Z., Shang, D., Tan, Z., Wang, Y., Le Breton, M., Zhu, W., Lou, S., Tang, M., Wu, Y., Zheng, J., Zeng, L., Hallquist, M., Hu, M., and Zhang, Y.: Efficient N_2O_5 Uptake and NO_3 Oxidation in the Outflow of Urban Beijing, Atmos. Chem. Phys. Discuss., 2018, 1-27, 10.5194/acp-2018-88, 2018.

Wang, M., Zeng, L., Lu, S., Shao, M., Liu, X., Yu, X., Chen, W., Yuan, B., Zhang, Q., Hu, M., and Zhang, Z.: Development and validation of a cryogen-free automatic gas chromatograph system (GC-MS/FID) for online measurements of volatile organic compounds, Anal Methods, 6, 9424-9434, 10.1039/C4AY01855A, 2014.

Wang, S., Shi, C., Zhou, B., Zhao, H., Wang, Z., Yang, S., and Chen, L.: Observation of NO_3 radicals over Shanghai, China, Atmos. Environ., 70, 401-409, https://doi.org/10.1016/j.atmosenv.2013.01.022, 2013.

Wang, T., Tham, Y. J., Xue, L. K., Li, Q. Y., Zha, Q. Z., Wang, Z., Poon, S. C. N., Dube, W. P., Blake, D. R., Louie, P. K. K., Luk, C. W. Y., Tsui, W., and Brown, S. S.: Observations of nitryl chloride and modeling its source and effect on ozone in the planetary boundary layer of southern China, J. Geophys. Res.-Atmos., 121, 2476-2489, 10.1002/2015JD024556, 2016.

Wang, X., Wang, H., Xue, L., Wang, T., Wang, L., Gu, R., Wang, W., Tham, Y. J., Wang, Z., Yang, L., Chen, J., and Wang, W.: Observations of N_2O_5 and $ClNO_2$ at a polluted urban surface site in North China: High N_2O_5 uptake coefficients and low $ClNO_2$ product yields, Atmos. Environ., 156, 125-134, https://doi.org/10.1016/j.atmosenv.2017.02.035, 2017.

Wang, Y., Chen, Z., Wu, Q., Liang, H., Huang, L., Li, H., Lu, K., Wu, Y., Dong, H., Zeng, L., and Zhang, Y.: Observation of atmospheric peroxides during Wangdu Campaign 2014 at a rural site in the North China Plain, Atmos. Chem. Phys., 16, 10985-11000, 10.5194/acp-16-10985-2016, 2016.

Wang, Z., Wang, W., Tham, Y. J., Li, Q., Wang, H., Wen, L., Wang, X., and Wang, T.: Fast heterogeneous N_2O_5 uptake and $ClNO_2$ production in power plant and industrial plumes observed in the nocturnal residual layer over the North China Plain, Atmos. Chem. Phys., 17, 12361-12378, 10.5194/acp-17-12361-2017, 2017.

Wexler, A. S., and Clegg, S. L.: Atmospheric aerosol models for systems including the ions H^+, NH_4^+, Na^+, SO_4^{2-}, NO_3^-,Cl^-, Br^-, and H_2O, J. Geophys. Res.-Atmos., 107, 10.1029/2001jd000451, 2002.

Wu, Z. J., Ma, N., Größ, J., Kecorius, S., Lu, K. D., Shang, D. J., Wang, Y., Wu, Y. S., Zeng, L. M., Hu, M., Wiedensohler, A., and Zhang, Y. H.: Thermodynamic properties of nanoparticles during new particle formation events in the atmosphere of North China Plain, Atmos. Res., 188, 55-63, https://doi.org/10.1016/j.atmosres.2017.01.007, 2017.

Yuan, B., Liu, Y., Shao, M., Lu, S. H., and Streets, D. G.: Biomass burning contributions to ambient VOCs species at a receptor site in the Pearl River Delta (PRD), China, Environ. Sci. Technol., 44, 4577-4582, 10.1021/es1003389, 2010.

Yun, H., Wang, T., Wang, W., Tham, Y. J., Li, Q., Wang, Z., and Poon, S. C. N.: Nighttime NOx loss and ClNO2 formation in the residual layer of a polluted region: Insights from field measurements and an iterative box model, Sci. Total Environ., 622-623, 727-734, 10.1016/j.scitotenv.2017.11.352, 2017.

Table 1: N_2O_5 uptake coefficients and $ClNO_2$ production yields from 10 selected plumes at Wangdu during the summer of 2014. The uncertainty (±) of the $\gamma(N_2O_5)$ and ϕ was estimated by the geometric mean of uncertainty from the scattering of the data plots and uncertainty from the measurement of N_2O_5, $ClNO_2$, aerosol surface area, and total NO_3^-.

Plume	Date (Time)	$\gamma(N_2O_5)$	$\phi(ClNO_2)$
1	20 June (23:00) – 21 June (01:20)	0.032 ± 0.011	0.48 ± 0.17
2	21 June (03:30 – 05:00)	0.030 ± 0.015	1.04 ± 0.35
3	24 June (20:30 – 22:10)	0.013 ± 0.006	0.09 ± 0.05
4	24 June (22:30) – 25 June (00:00)	0.025 ± 0.008	0.44 ± 0.13
5	27 June (20:40) – 28 June (00:00)	0.012 ± 0.007	0.14 ± 0.08
6	28 June (22:30) – 29 June (00:40)	0.005 ± 0.002	0.20 ± 0.06
7	29 June (22:00) – 30 June (01:20)	0.012 ± 0.004	0.36 ± 0.15
8	30 June (21:10) – 1 July (00:10)	0.015 ± 0.006	0.21 ± 0.07
9	5 July (00:30) – 5 July (02:30)	0.039 ± 0.020	0.43 ± 0.26
10	5 July (23:40) – 6 July (02:00)	0.033 ± 0.015	0.06 ± 0.03

Table 2: Summary of field-observed N_2O_5 uptake coefficient and $ClNO_2$ yield from previous studies.

Location	Environment	$\gamma(N_2O_5)$	ϕ	Descriptions	Reference
North America					
New England, US	Coastal + Inland	0.001–0.017	*n.a*	Aircraft measurement (below 1500 m). $\gamma(N_2O_5)$ is higher in elevated sulfate region.	Brown et al., 2006
Coast of Texas, US	Coastal	*n.a*	0.10–0.65	Shipborne measurement. Influenced by urban outflow.	Osthoff et al., 2008
Texas, US	Coastal + Inland	0.0005–0.006	*n.a*	Aircraft measurement (below 1000 m). $\gamma(N_2O_5)$ was independent of humidity (RH, 34% to 85%) and aerosol compositions.	Brown et al., 2009
Seattle, US	Coastal	0.005–0.04	*n.a*	Urban/suburban environment. $\gamma(N_2O_5)$ was enhanced with higher RH but has a strong correlation with the organic-to-sulfate ratio.	Bertram et al., 2009
Calgary, Canada	Inland	0.02	0.15	Ground urban area. Influenced by anthropogenic activities within the urban area.	Mielke et al., 2011
La Jolla, US	Coastal	0.001–0.029	*n.a*	Polluted coastal site. $\gamma(N_2O_5)$ was suppressed by nitrate.	Riedel et al., 2012b
Coast of Los Angeles, US	Coastal	*n.a*	0.15–0.62	Shipborne measurement. Influenced by the land-sea breeze.	Wagner et al., 2012
Pasadena, US	Coastal	$\gamma\phi = 0.008$ (average)		Ground measurement during the California Nexus 2010 campaign. $\gamma\phi$ was enhanced by submicron chloride, but suppressed by organic matter and liquid water content.	Mielke et al., 2013
Boulder, US	Inland	0.002–0.1	0.01–0.98	Tower measurement (0-300 m) downwind of an urban area. $\gamma(N_2O_5)$ dependence on nitrate. Higher ϕ in coal combustion plume.	Wagner et al., 2013 Riedel et al., 2013
Europe					
London	Coastal + Inland	0.01–0.03	*n.a*	Aircraft measurement (500-1000 m). $\gamma(N_2O_5)$ was independent of humidity (RH, 50% to 90%) but dependent on nitrate loading.	Morgan et al., 2015
Kleiner Feldberg	Inland	0.004–0.11	0.029–1.38	Semi-rural mountain-top site in SW Germany (825 m above sea level). $\gamma(N_2O_5)$ was independent of aerosol compositions but has a weak dependence on humidity.	Phillips et al., 2016

China					
Hong Kong	Coastal	0.004–0.021	0.02–0.98	Rural mountain-top site in southern China (957 m above sea level). Influenced by pollution from the urban area.	Brown et al., 2016 Yun et al., 2018
Jinan	Inland	0.042–0.092	0.01–0.08	Urban-surface in the polluted urban area of northern China. $\gamma(N_2O_5)$ showed positive dependence on RH.	Wang X. et al., 2017
Mt. Tai	Inland	0.021–0.103	0.17–0.90	Mountaintop site in northern China (1465 m above sea level). Elevated $\gamma(N_2O_5)$ for high humidity (>80%) condition. Higher ϕ in coal-fired power plant plumes.	Wang Z. et al., 2017
Beijing-urban	Inland	0.025−0.072	*n.a*	Polluted urban surface-site in northern China during early autumn. High $\gamma(N_2O_5)$ was related to high aerosol liquid water content.	Wang H. et al., 2017
Beijing-rural	Inland	0.012–0.055	0.50–1.00	Rural surface site in northern Beijing. Influenced by the outflow of the urban Beijing.	Wang H. et al., 2018
Wangdu	Inland	0.005–0.039	0.06–1.04	Semi-rural and surface site in northern China. $\gamma(N_2O_5)$ has a strong dependence on humidity and aerosol water content. Variable ϕ and lower values for cases influenced by biomass burning activities.	This study

n.a = no information available

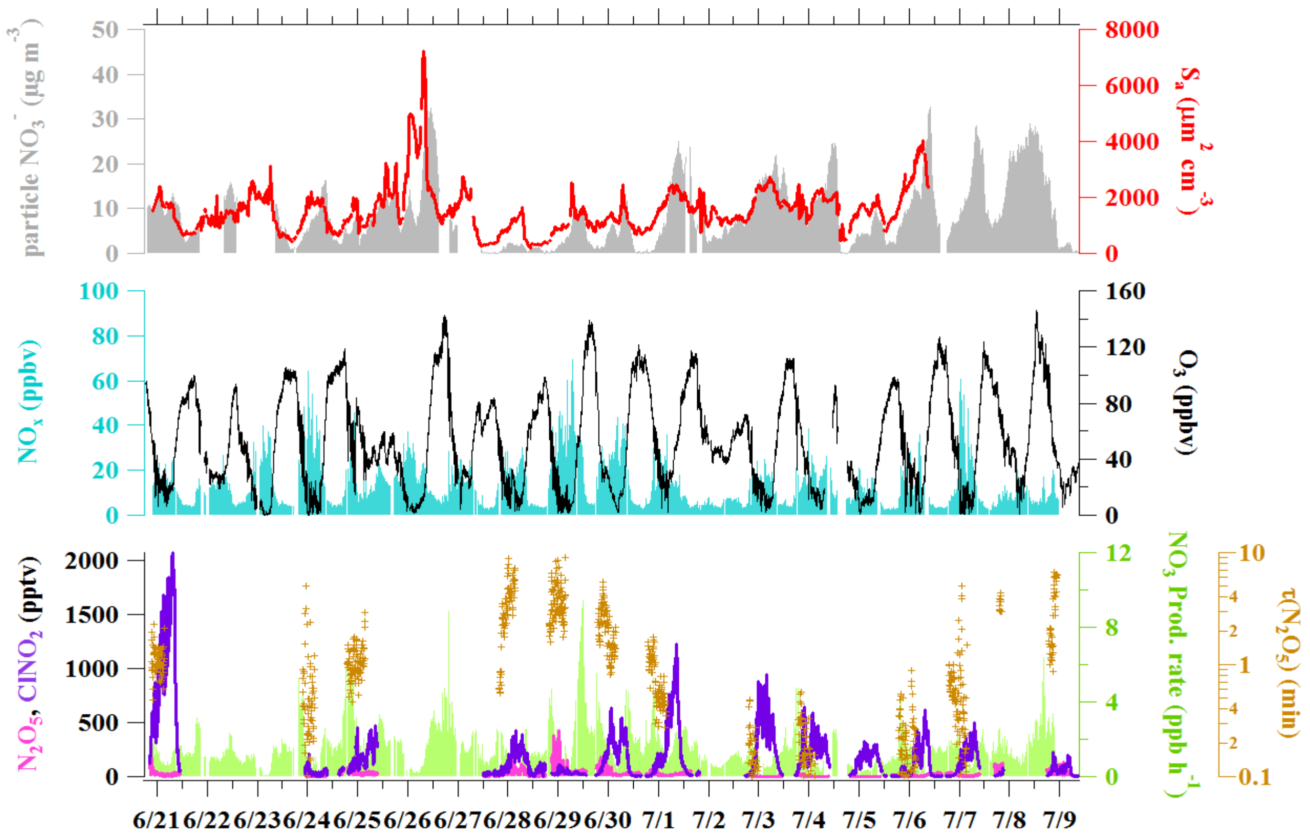

Figure 1: Time series of N_2O_5, $ClNO_2$, NO_3 production rate, the steady-state lifetime of N_2O_5, O_3, NO_x, fine particulate NO_3^-, and S_a data at Wangdu from 21 June to 9 July 2014. N_2O_5 and $ClNO_2$ are 1-min data, whereas the NO_x, O_3, NO_3 production rate and $\tau(N_2O_5)$ are given as 5-min averages. The data for S_a and fine particulate NO_3^- are in 10-min and 30-min time resolutions, respectively. The data gaps were caused by technical problems, calibrations, or instrument maintenance.

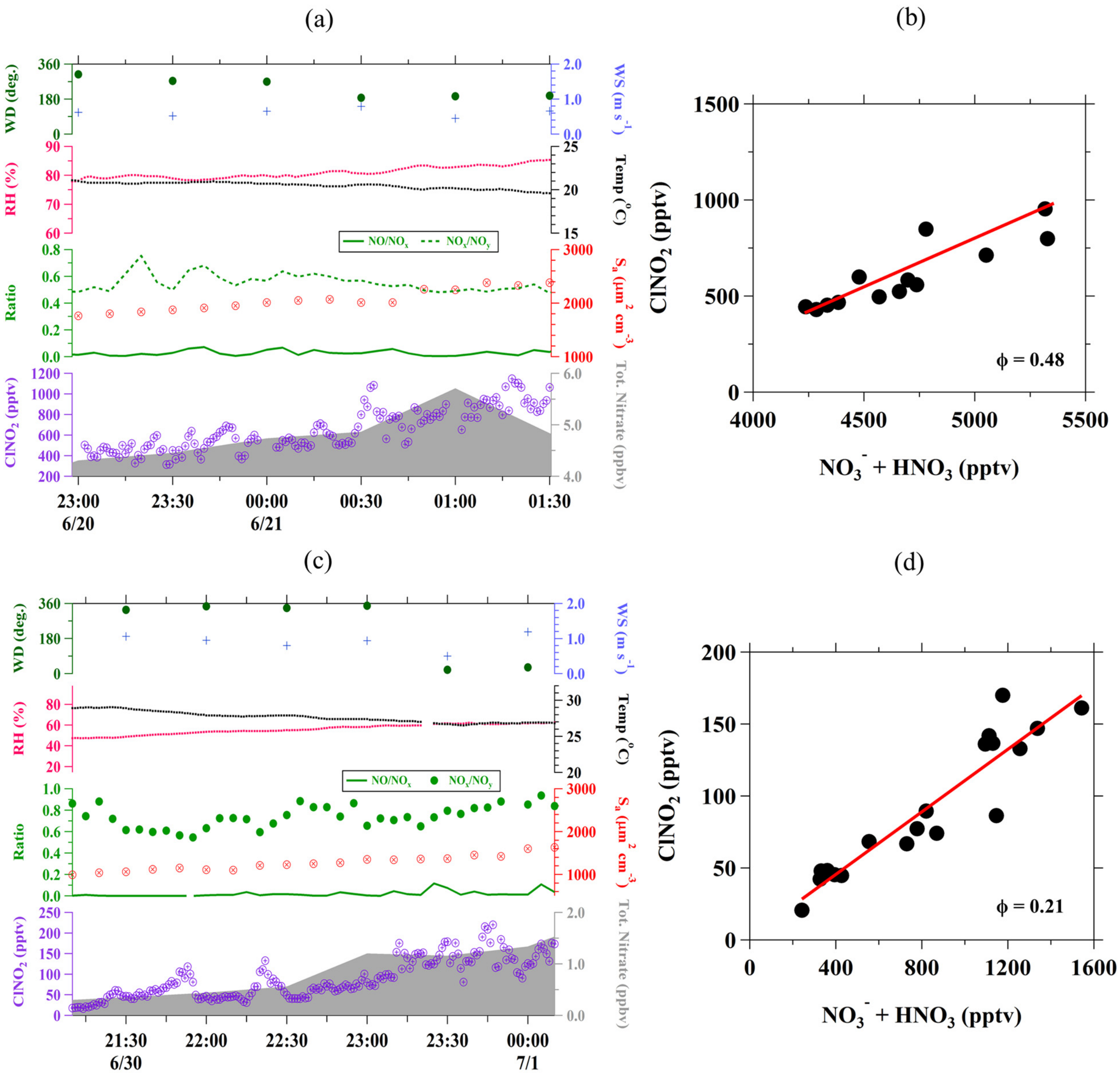

Figure 2: Example of the accumulation of $ClNO_2$ and total nitrate (particulate NO_3^- + HNO_3) concentrations during the relatively constant condition of relevant chemical compositions and environmental variables observed for (a) Plume 1 on 20-21 June 2014 and (c) Plume 7 on 29-30 June 2014. Scatter plots of $ClNO_2$ versus particulate NO_3^- + HNO_3 to estimate the $ClNO_2$ yield (ϕ) for these two cases are shown in (c) and (d).

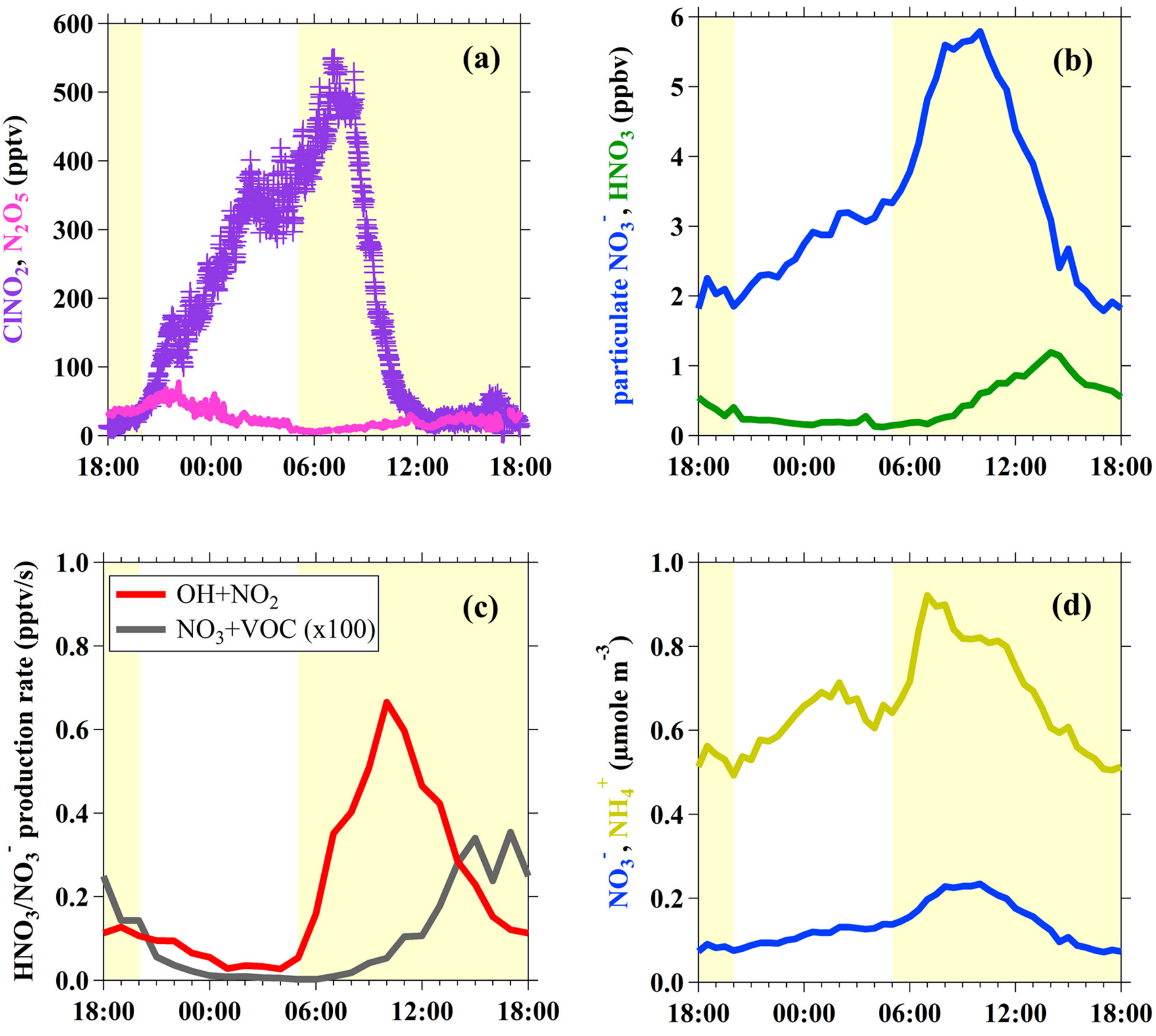

Figure 3: Diurnal variations of (a) N_2O_5 and $ClNO_2$; b) particulate NO_3^- and gas-phase HNO_3 (c) gas-phase production rate of NO_3^-/HNO_3 via reaction of OH+NO_2 and NO_3+VOC; and (d) concentrations of NH_4^+ in relation to particulate NO_3^-. The time indicated in the x-axis is the local time and the shaded area (yellow) represent the daytime.

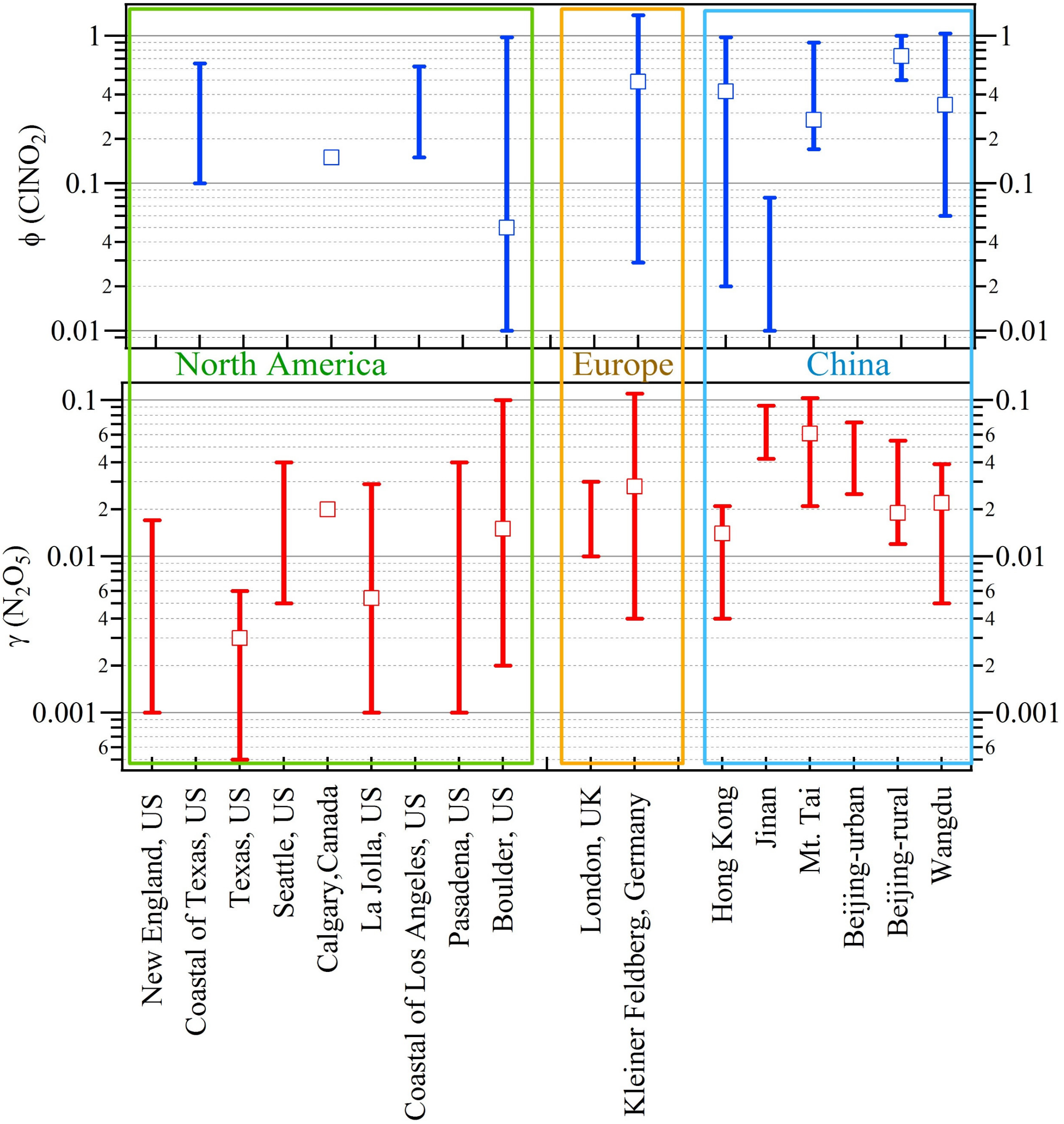

Figure 4: Comparison of the field-observed N_2O_5 uptake coefficient and $ClNO_2$ yield from previous studies. Sticks represent the range of the reported values, and cubes represent the median or average values reported in these measurements. The corresponding references are listed in Table 2.

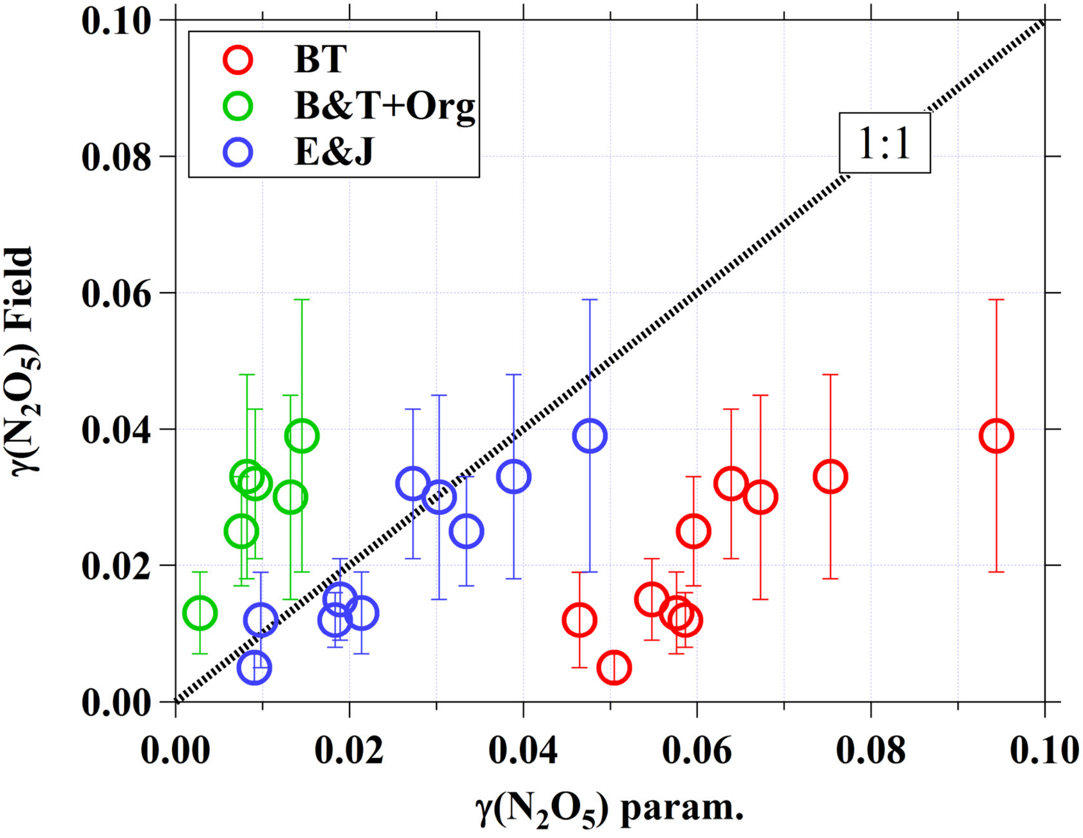

Figure 5: Comparison of field-derived N_2O_5 uptake coefficients with values computed from different parameterizations. The dashed line represents 1:1, and the error bars show the uncertainty of $\gamma(N_2O_5)$ derived from the field.

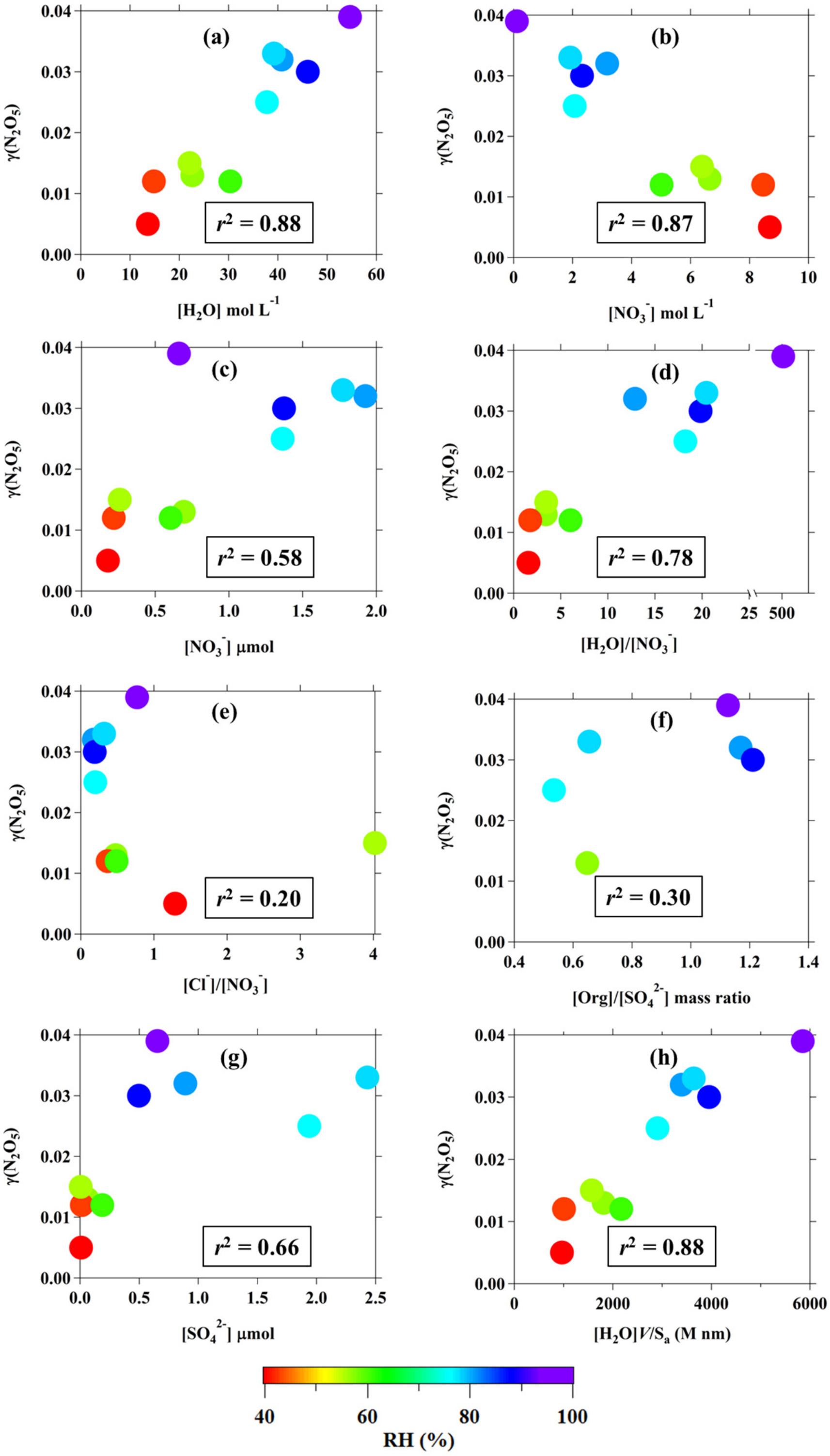
(a)
$r^2 = 0.88$
$\gamma(N_2O_5)$
0.00
0.01
0.02
0.03
0.04
0
10
20
30
40
50
60
$[H_2O]$ mol L^{-1}
(b)
$r^2 = 0.87$
$\gamma(N_2O_5)$
0
2
4
6
8
10
$[NO_3^-]$ mol L^{-1}
(c)
$r^2 = 0.58$
$\gamma(N_2O_5)$
0.0
0.5
1.0
1.5
2.0
$[NO_3^-]$ µmol
(d)
$r^2 = 0.78$
$\gamma(N_2O_5)$
0
5
10
15
20
25
500
$[H_2O]/[NO_3^-]$
(e)
$r^2 = 0.20$
$\gamma(N_2O_5)$
0
1
2
3
4
$[Cl^-]/[NO_3^-]$
(f)
$r^2 = 0.30$
$\gamma(N_2O_5)$
0.4
0.6
0.8
1.0
1.2
1.4
$[Org]/[SO_4^{2-}]$ mass ratio
(g)
$r^2 = 0.66$
$\gamma(N_2O_5)$
0.0
0.5
1.0
1.5
2.0
2.5
$[SO_4^{2-}]$ µmol
(h)
$r^2 = 0.88$
$\gamma(N_2O_5)$
0
2000
4000
6000
$[H_2O]V/S_a$ (M nm)
40
60
80
100
RH (%)

Figure 6: Relationship between field-derived γ(N_2O_5) and a) aerosol water content (mol per volume of aerosol); b) nitrate concentration per volume of aerosol; c) particulate nitrate concentration (μmol m^{-3} of air); d) H_2O to NO_3^- molar ratio; e) Cl^- to NO_3^- molar ratio; f) organic-to-sulfate mass ratio (data from aerosol mass spectrometer); g) concentration of SO_4^{2-} (μmol m^{-3} of air); and h) amount of water in aerosol multiplied by the volume-to-surface area ratio. Color code represents the ambient RH, and the value in the box is the best correlation coefficient obtained from curve fittings.

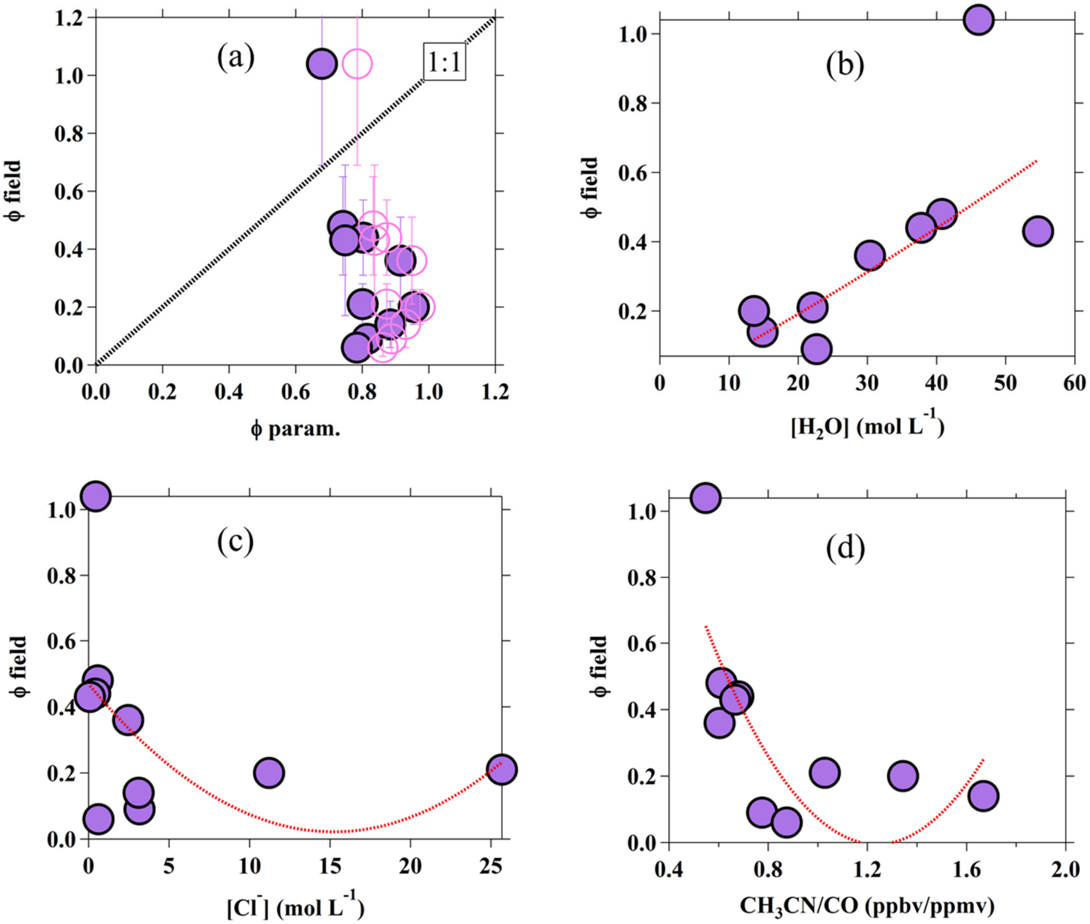

Figure 7: Scatter plots for (a) yield derived from the field versus yield calculated from the parameterization, using k_{R4}/k_{R3} of 483 (recommended by Bertram and Thornton, 2009; solid circle) and 836 (recommended by Behnke et al., 1997; pink open circle). Error bars represent the uncertainty of field-derived ϕ, and the black dotted line represents the 1:1 ratio); (b) field-derived yield versus aerosol water content; (c) field-derived yield versus chloride; and (d) field-derived yield versus CH_3CN/CO. The red dotted line shows the quadratic fitting line of the data.